THE LANCET
Planetary Health

## Supplementary appendix

This appendix formed part of the original submission and has been peer reviewed. We post it as supplied by the authors.

Supplement to: Madaniyazi L, Armstrong B, Tobias A, et al. Seasonality of mortality under climate change: a multicountry projection study. *Lancet Planet Health* 2024; **8:** e86–94.

**Supplementary Material**

Seasonality of mortality under climate change: a multicountry projection study

# Table of Contents

Detailed information on the analytical framework ..... 1

Table S1. Peak* (empirical 95% confidence intervals) by decades for each climatic zone under scenarios 4

Table S2. Trough* (empirical 95% confidence intervals) by decades for each climatic zone scenarios ..... 6

Table S3. Peak-to-trough ratio (95% confidence intervals) by decades for each climatic zone under scenarios ..... 8

Table S4. Attributable fraction (95% empirical confidence intervals) by decades for each climatic zone under scenarios ..... 10

Figure S1. Seasonality of mortality in each country/area from the 2000s to 2090s under four scenarios .. 12

Figure S2. Temporal changes in the size of seasonality by country/are under four scenarios ..... 35

**Detailed information on the analytical framework**

The analytical framework is described below. Part of the statistical analysis is based on previously published methods, applied in a previous seasonality assessment[1] using the same dataset and then summarized in a recent tutorial.[2]

**Observed series:**

Historical data on temperature and mortality were collected via the Multi-Country Multi-City (MCC) Collaborative Research Network (http://mccstudy.lshtm.ac.uk/). The dataset is composed of observed daily time series for daily mean temperature $Temp.obs$ and mortality counts $Mort.obs$ for all causes or non-external causes (the International Classification of Diseases (ICD): A00-R99 for 10th ICD and 001–799 for 9th ICD). The data covers 707 locations across 43 countries/areas in largely overlapping periods from 1 January 1969 to 31 December 2020.

**Modeled series:**

The modeled data on daily mean temperature $Temp.mol$ were collected for the period of 1969- 2099 from the database developed in the Inter-Sectoral Impact Model Intercomparison Project (ISIMIP 3b). We selected four scenarios under the Shared Socioeconomic Pathways (SSP) within Phase 6 of the Coupled Model Intercomparison Project (SSP1-2.6, SSP2-4.5, SSP3-7.0, and SSP5-8.5),[3,4] representing a range of scenarios for climate change from mild (SSP1-2.6) to extreme (SSP5-8.5). The data under each scenario includes simulations from five general circulation models (GCMs), including GFDL-ESM4, IPSL-CM6A-LR, MPI-ESM1-2-HR, MRI-ESM2-0, and UKESM1-0-LL. We extracted the modeled data for each MCC location by linking each location's coordinates with the corresponding GCM grid-cell from the simulation in 1969-2099. To preserve the trend and variability of the original data in the observed series, we recalibrated the $Temp_{mod}$ series using the observed $T_{obs}$ series and obtained $Temp^{*}_{mod}$.[5]

**Statistical analysis**

***Projecting the daily mortality***

We fitted a quasi-Poisson regression model to the observed mortality series $Mort.obs$: [6]

$$\log[E(Mort.obs_t)] = \alpha + cs(doy_t) + [LTT\ fn](t) + cb\big(Temp.obs_{t,l}\big) \qquad (1)$$

Where $Mort.obs_t$ is the mortality count on day *t* from the observed series; *cs* is a cyclic spline of day-of-year ($doy$) on day *t* with 4 degrees of freedom (*df*) to fit the baseline seasonality (that remaining after temperature effects were modelled); *LTT fn* is a natural cubic spline of the day *t* with 2 *df* per decade to fit the long-term trend ($LTT$); *cb* is a bi-dimensional cross-basis function for the non-linear and delayed exposure-lag-response association of $Mort.obs_t$ with the observed daily mean temperature $Temp.obs_t$ up to 21 days, and *l* is the lag days. For the cross-basis function, a natural cubic spline for exposure-response curve with three internal knots placed at the 10th, 75th, and 90th percentiles of location-specific temperature distributions, and another natural cubic spline for lag-response curve with 21 days of lags with an intercept and three internal knots placed at equally spaced values in the log scale.[6,7]
Next, we obtained model parameters from the fitted model (1) and projected the daily mortality $Mort.proj_{t^*}$ on day $t^*$ from 2000 to 2099:

$$E(Mort.proj_{t^*}) = exp\left(\hat{\alpha} + \hat{cs}(doy_{t^*}) + [\widehat{LTT\ fn}](t_{base}) + \widehat{cb}\big(Temp.mod_{t^*,l}\big)\right) \qquad (2)$$

Where $Mort.proj_{t^*}$ is the projected daily mortality on day $t^*$ from 2000 to 2099; $\hat{a}$, $\widehat{cs}$, $\widehat{LTT\,fn}$ , and $\widehat{cb}$ are the model parameters obtained from the fitted model (1) above; $doy_{t^*}$ is the day-of-year from 2000 to 2099; $t_{base}$ is a baseline time value we set on a certain date to fix the *LTT,* and $t_{base}$ can be different between locations, as the observation periods vary between locations; $Temp.mod_{t^*}$ is the daily mean temperature from the recalibrated modelled series from 2000 to 2099. Here, by using the model parameter $\widehat{cb}$ from the fitted model (1), we assumed a constant association between temperature and mortality and did not consider potential adaptation to changing climate. In addition, we also assumed the baseline seasonality exp ($\widehat{cs}(doy_{t^*})$) does not change from 2000 to 2099.

We computed $Mort.proj_{t^*}$ for each location and combinations of GCMs and SSPs, and the average across five GCMs for each SSP ($\overline{Mort.proj}_{t^*}$) was used for the seasonality assessment in the next step.

***Assessing seasonality***

We fitted a cyclic spline of $doy_{t^*}$ with 4 *df* to the projected $\overline{Mort.proj}_{t^*}$ to assess its seasonality for each location, by extending a method previously described.[1,2]

$$\log[E(\overline{Mort.proj}_{t^*})] = \alpha + cs(doy_{t^*}) \qquad (3)$$

Where $\overline{Mort.proj}_{t^*}$ is the average of projected daily mortality across five GCMs on day $t^*$ from 2000 to 2099; *cs* is a cyclic spline of day-of-year ($doy_{t^*}$) with 4 *df* to fit the seasonality; $doy_{t^*}$ ranges from 1 to 365 corresponding to 1 January through to 31 December for locations in the northern hemisphere and 1 July to 30 June of the following year for locations in the southern hemisphere. From the coefficients of $cs(doy_{t^*})$, we derived the log relative risk $\beta_{doy}$ of mortality on each $doy$ compared with the minimum mortality.

The coefficients of $cs(doy_{t^*})$ from location-specific seasonality assessment were pooled by each climate zone (location nested within the country/area as random effects) and country/area (location as a random effect), respectively, using the multivariate meta-analysis.

The key features of seasonality include its shape, timings (peak and trough) and size (amplitude and impact):

- The shape can be estimated through the fitted seasonal curve from the regression model (3), and described by visual inspection.
- The $doy$ with maximum and minimum mortality estimates were identified from the fitted seasonal curve as the peak and trough, respectively. The empirical confidence intervals (eCIs) for peak and trough were obtained through Monte Carlo simulations.[8]
- We summarized the size of seasonality by measuring the amplitude and estimating its impact on mortality. The amplitude was measured as the ratio of the maximum mortality estimate at peak day to the minimum mortality estimate at trough day (i.e. peak-to-trough ratio, PTR): $PTR = \exp(\beta_{peak}/\beta_{trough})$, and its 95% CI was obtained from the variance matrix of the estimated coefficients from the $cs(doy_{t^*})$. Then, we obtained the *AF* as: $AF = \sum p_{doy}[1 - \exp(\beta_{doy})]$, where $p_{doy}$ is the percentage of cases on each $doy$ . The eCIs for AF were estimated through Monte Carlo simulations.[9] Here, the AF estimates the fraction by which mortality would be reduced in a counterfactual scenario where mortality risk never rose above its seasonal trough.
  We estimated the change in PTR and AF, denoted as $d$, by decades in comparison with 2000-09, respectively. The formular are as follows: $d = \widehat{E_{decade}} - \widehat{E_{2000-09}}$ and $SE(d) = \sqrt{\widehat{SE^2_{decade}} + \widehat{SE^2_{2000-09}}}$, where $\hat{E}$ are the estimates of log(PTR) and AF in the future decades (from the 2010s to the 2100s) and the current decade (i.e., 2000-09), and $\widehat{SE}$ are their respective standard

errors. We report the relative change in PTR by taking the exponentiation of the difference in log(PTR).

References:


1 Madaniyazi L, Armstrong B, Chung Y, *et al.* Seasonal variation in mortality and the role of temperature: a multi-country multi-city study. *Int J Epidemiol* 2022; **51**: 122–33.
2 Madaniyazi L, Tobias A, Kim Y, Chung Y, Armstrong B, Hashizume M. Assessing seasonality and the role of its potential drivers in environmental epidemiology: a tutorial. *Int J Epidemiol* 2022; **51**: 1677–86.
3 Riahi K, van Vuuren DP, Kriegler E, *et al.* The Shared Socioeconomic Pathways and their energy, land use, and greenhouse gas emissions implications: An overview. *Global Environmental Change* 2017; **42**: 153–68.
4 O'Neill BC, Tebaldi C, van Vuuren DP, *et al.* The Scenario Model Intercomparison Project (ScenarioMIP) for CMIP6. *Geosci Model Dev* 2016; **9**: 3461–82.
5 Vicedo-Cabrera AM, Sera F, Gasparrini A. Hands-on Tutorial on a Modeling Framework for Projections of Climate Change Impacts on Health. *Epidemiology* 2019; **30**: 321–9.
6 Gasparrini A, Guo Y, Hashizume M, *et al.* Mortality risk attributable to high and low ambient temperature: a multicountry observational study. *Lancet* 2015; **386**: 369–75.
7 Gasparrini A, Armstrong B, Kenward MG. Distributed lag non-linear models. *Stat Med* 2010; **29**: 2224–34.
8 Tobías A, Armstrong B, Gasparrini A. Brief report: Investigating uncertainty in the minimum mortality temperature. *Epidemiology* 2017; **28**: 72–6.
9 Gasparrini A, Leone M. Attributable risk from distributed lag models. BMC Med Res Methodol 2014; 14, 55. http://www.biomedcentral.com/1471-2288/14/55.

**Table S1**. Peak* (empirical 95% confidence intervals) by decades for each climatic zone under scenarios

| Decades | SSP1-2.6 | SSP2-4.5 | SSP3-7.0 | SSP5-8.5 |
|---|---|---|---|---|
| Tropical | | | | |
| 2000s | 29 ( 222 , 72 ) | 29 ( 221 , 72 ) | 29 ( 221 , 72 ) | 29 ( 221 , 72 ) |
| 2010s | 40 ( 226 , 218 ) | 37 ( 224 , 206 ) | 41 ( 227 , 221 ) | 35 ( 224 , 76 ) |
| 2020s | 56 ( 243 , 236 ) | 52 ( 238 , 233 ) | 50 ( 236 , 232 ) | 51 ( 237 , 232 ) |
| 2030s | 60 ( 249 , 240 ) | 60 ( 247 , 240 ) | 62 ( 254 , 241 ) | 66 ( 262 , 244 ) |
| 2040s | 64 ( 263 , 241 ) | 65 ( 257 , 243 ) | 73 ( 263 , 250 ) | 73 ( 329 , 238 ) |
| 2050s | 72 ( 278 , 245 ) | 72 ( 358 , 236 ) | 74 ( 5 , 235 ) | 79 ( 27 , 234 ) |
| 2060s | 70 ( 264 , 247 ) | 77 ( 19 , 233 ) | 81 ( 60 , 147 ) | 86 ( 67 , 223 ) |
| 2070s | 70 ( 267 , 246 ) | 80 ( 35 , 233 ) | 87 ( 71 , 229 ) | 94 ( 72 , 221 ) |
| 2080s | 70 ( 280 , 245 ) | 83 ( 41 , 229 ) | 88 ( 69 , 149 ) | 87 ( 66 , 228 ) |
| 2090s | 66 ( 263 , 244 ) | 86 ( 65 , 224 ) | 80 ( 58 , 225 ) | 82 ( 65 , 225 ) |
| Arid | | | | |
| 2000s | 9 ( 1 , 17 ) | 9 ( 1 , 17 ) | 9 ( 1 , 17 ) | 9 ( 1 , 17 ) |
| 2010s | 9 ( 1 , 17 ) | 9 ( 1 , 17 ) | 9 ( 1 , 17 ) | 9 ( 1 , 17 ) |
| 2020s | 9 ( 1 , 16 ) | 9 ( 1 , 17 ) | 9 ( 1 , 16 ) | 9 ( 364 , 17 ) |
| 2030s | 9 ( 1 , 16 ) | 8 ( 364 , 17 ) | 8 ( 364 , 16 ) | 8 ( 364 , 16 ) |
| 2040s | 9 ( 364 , 17 ) | 8 ( 364 , 16 ) | 8 ( 363 , 16 ) | 9 ( 364 , 16 ) |
| 2050s | 8 ( 364 , 16 ) | 8 ( 363 , 16 ) | 9 ( 363 , 17 ) | 9 ( 363 , 17 ) |
| 2060s | 8 ( 364 , 16 ) | 8 ( 363 , 16 ) | 9 ( 362 , 18 ) | 9 ( 223 , 18 ) |
| 2070s | 8 ( 364 , 16 ) | 9 ( 363 , 18 ) | 9 ( 352 , 18 ) | 9 ( 215 , 18 ) |
| 2080s | 8 ( 364 , 16 ) | 9 ( 362 , 17 ) | 9 ( 216 , 18 ) | 9 ( 212 , 16 ) |
| 2090s | 8 ( 364 , 16 ) | 9 ( 360 , 17 ) | 9 ( 213 , 17 ) | 214 ( 211 , 14 ) |
| Temperate | | | | |
| 2000s | 18 ( 14 , 21 ) | 18 ( 14 , 21 ) | 17 ( 14 , 21 ) | 18 ( 14 , 21 ) |
| 2010s | 18 ( 14 , 22 ) | 18 ( 14 , 22 ) | 18 ( 14 , 22 ) | 18 ( 15 , 22 ) |
| 2020s | 18 ( 14 , 22 ) | 18 ( 15 , 22 ) | 17 ( 14 , 21 ) | 19 ( 15 , 23 ) |
| 2030s | 18 ( 15 , 22 ) | 18 ( 15 , 22 ) | 19 ( 15 , 22 ) | 18 ( 15 , 22 ) |
| 2040s | 18 ( 15 , 22 ) | 18 ( 14 , 22 ) | 17 ( 14 , 22 ) | 18 ( 14 , 22 ) |
| 2050s | 18 ( 14 , 22 ) | 18 ( 14 , 22 ) | 18 ( 14 , 22 ) | 18 ( 14 , 21 ) |
| 2060s | 18 ( 15 , 22 ) | 18 ( 14 , 22 ) | 19 ( 15 , 22 ) | 19 ( 15 , 23 ) |
| 2070s | 18 ( 14 , 21 ) | 19 ( 15 , 23 ) | 18 ( 14 , 22 ) | 18 ( 212 , 22 ) |
| 2080s | 18 ( 14 , 22 ) | 18 ( 14 , 21 ) | 18 ( 213 , 22 ) | 214 ( 211 , 19 ) |
| 2090s | 18 ( 15 , 22 ) | 18 ( 15 , 22 ) | 214 ( 211 , 22 ) | 214 ( 212 , 215 ) |
| Continental | | | | |
| 2000s | 22 ( 15 , 31 ) | 22 ( 15 , 31 ) | 22 ( 15 , 31 ) | 22 ( 15 , 31 ) |
| 2010s | 22 ( 15 , 32 ) | 22 ( 16 , 32 ) | 22 ( 15 , 32 ) | 23 ( 17 , 32 ) |
| 2020s | 22 ( 15 , 33 ) | 22 ( 16 , 32 ) | 22 ( 16 , 32 ) | 23 ( 16 , 32 ) |

| | | | | |
|---|---|---|---|---|
| 2030s | 22 ( 16 , 31 ) | 22 ( 15 , 33 ) | 23 ( 16 , 32 ) | 23 ( 17 , 32 ) |
| 2040s | 21 ( 15 , 30 ) | 20 ( 14 , 30 ) | 21 ( 14 , 31 ) | 21 ( 15 , 30 ) |
| 2050s | 21 ( 15 , 30 ) | 21 ( 15 , 31 ) | 20 ( 13 , 30 ) | 21 ( 14 , 30 ) |
| 2060s | 22 ( 15 , 31 ) | 21 ( 15 , 30 ) | 22 ( 14 , 32 ) | 21 ( 14 , 31 ) |
| 2070s | 20 ( 13 , 31 ) | 21 ( 14 , 31 ) | 20 ( 13 , 31 ) | 19 ( 210 , 29 ) |
| 2080s | 21 ( 14 , 30 ) | 21 ( 14 , 31 ) | 20 ( 214 , 30 ) | 211 ( 206 , 26 ) |
| 2090s | 22 ( 15 , 32 ) | 21 ( 14 , 30 ) | 19 ( 208 , 30 ) | 212 ( 207 , 24 ) |

*The $day - of - year$ with maximum mortality estimates were identified from the fitted seasonal curve as the peak. The empirical confidence intervals (eCIs) for peak and trough were obtained through Monte Carlo simulations. These estimates are obtained by pooling location-specific estimates for each climate zone. We removed Feb 29 from the datasets and took values from 1 to 365 to represent the day-of-year, corresponding to 1 January through 31 December for locations in the northern hemisphere and 1 July to 30 June of the following year for locations in the southern hemisphere.

**Table S2**. Trough* (empirical 95% confidence intervals) by decades for each climatic zone scenarios

| Decades | SSP1-2.6 | SSP2-4.5 | SSP3-7.0 | SSP5-8.5 |
|---|---|---|---|---|
| Tropical | | | | |
| 2000s | 142 ( 342 , 316 ) | 142 ( 341 , 315 ) | 142 ( 343 , 316 ) | 142 ( 342 , 316 ) |
| 2010s | 144 ( 338 , 320 ) | 143 ( 337 , 320 ) | 144 ( 337 , 321 ) | 143 ( 338 , 319 ) |
| 2020s | 147 ( 335 , 326 ) | 146 ( 335 , 325 ) | 145 ( 334 , 324 ) | 146 ( 334 , 325 ) |
| 2030s | 147 ( 335 , 326 ) | 147 ( 335 , 326 ) | 148 ( 335 , 327 ) | 151 ( 338 , 331 ) |
| 2040s | 313 ( 136 , 125 ) | 149 ( 336 , 329 ) | 338 ( 160 , 155 ) | 331 ( 151 , 148 ) |
| 2050s | 324 ( 145 , 139 ) | 323 ( 146 , 117 ) | 325 ( 146 , 137 ) | 338 ( 269 , 151 ) |
| 2060s | 330 ( 150 , 147 ) | 336 ( 157 , 153 ) | 339 ( 239 , 153 ) | 342 ( 290 , 1 ) |
| 2070s | 327 ( 147 , 144 ) | 336 ( 279 , 148 ) | 345 ( 302 , 1 ) | 348 ( 261 , 3 ) |
| 2080s | 326 ( 146 , 141 ) | 336 ( 275 , 148 ) | 343 ( 256 , 2 ) | 343 ( 232 , 2 ) |
| 2090s | 320 ( 141 , 135 ) | 344 ( 284 , 38 ) | 334 ( 232 , 2 ) | 334 ( 236 , 1 ) |
| Arid | | | | |
| 2000s | 255 ( 140 , 268 ) | 255 ( 141 , 268 ) | 255 ( 140 , 269 ) | 255 ( 141 , 268 ) |
| 2010s | 258 ( 138 , 271 ) | 258 ( 137 , 271 ) | 259 ( 135 , 272 ) | 258 ( 137 , 271 ) |
| 2020s | 262 ( 133 , 274 ) | 262 ( 135 , 274 ) | 263 ( 131 , 275 ) | 263 ( 130 , 275 ) |
| 2030s | 266 ( 129 , 277 ) | 266 ( 125 , 277 ) | 266 ( 124 , 277 ) | 267 ( 124 , 278 ) |
| 2040s | 267 ( 125 , 278 ) | 269 ( 120 , 279 ) | 270 ( 117 , 280 ) | 273 ( 118 , 283 ) |
| 2050s | 268 ( 123 , 279 ) | 271 ( 116 , 281 ) | 275 ( 113 , 284 ) | 279 ( 113 , 288 ) |
| 2060s | 268 ( 122 , 280 ) | 274 ( 114 , 284 ) | 280 ( 112 , 289 ) | 283 ( 109 , 292 ) |
| 2070s | 268 ( 122 , 279 ) | 277 ( 113 , 287 ) | 283 ( 109 , 292 ) | 124 ( 100 , 294 ) |
| 2080s | 267 ( 121 , 278 ) | 279 ( 110 , 288 ) | 125 ( 102 , 293 ) | 120 ( 96 , 298 ) |
| 2090s | 266 ( 123 , 278 ) | 281 ( 111 , 290 ) | 121 ( 97 , 297 ) | 116 ( 301 , 298 ) |
| Temperate | | | | |
| 2000s | 256 ( 225 , 263 ) | 256 ( 238 , 263 ) | 256 ( 240 , 264 ) | 256 ( 239 , 263 ) |
| 2010s | 262 ( 252 , 268 ) | 261 ( 251 , 268 ) | 261 ( 250 , 268 ) | 262 ( 236 , 268 ) |
| 2020s | 266 ( 258 , 271 ) | 267 ( 257 , 272 ) | 264 ( 254 , 270 ) | 268 ( 258 , 273 ) |
| 2030s | 271 ( 264 , 276 ) | 272 ( 265 , 277 ) | 272 ( 264 , 276 ) | 273 ( 267 , 278 ) |
| 2040s | 273 ( 265 , 278 ) | 276 ( 270 , 280 ) | 276 ( 269 , 280 ) | 279 ( 273 , 283 ) |
| 2050s | 274 ( 267 , 279 ) | 278 ( 272 , 282 ) | 282 ( 276 , 286 ) | 285 ( 279 , 288 ) |
| 2060s | 276 ( 270 , 280 ) | 281 ( 276 , 285 ) | 286 ( 281 , 290 ) | 290 ( 286 , 293 ) |
| 2070s | 275 ( 268 , 279 ) | 285 ( 279 , 288 ) | 289 ( 283 , 292 ) | 292 ( 288 , 295 ) |
| 2080s | 274 ( 267 , 278 ) | 285 ( 280 , 288 ) | 292 ( 287 , 295 ) | 296 ( 292 , 299 ) |
| 2090s | 272 ( 264 , 276 ) | 287 ( 281 , 290 ) | 295 ( 290 , 298 ) | 299 ( 295 , 302 ) |
| Continental | | | | |
| 2000s | 215 ( 193 , 224 ) | 215 ( 193 , 224 ) | 215 ( 193 , 224 ) | 215 ( 193 , 224 ) |
| 2010s | 215 ( 189 , 228 ) | 215 ( 190 , 228 ) | 215 ( 191 , 230 ) | 214 ( 188 , 230 ) |
| 2020s | 216 ( 180 , 239 ) | 216 ( 183 , 240 ) | 217 ( 184 , 241 ) | 216 ( 182 , 246 ) |

| | | | | |
|---|---|---|---|---|
| 2030s | 229 ( 175 , 258 ) | 235 ( 174 , 260 ) | 225 ( 175 , 255 ) | 238 ( 171 , 263 ) |
| 2040s | 248 ( 171 , 267 ) | 253 ( 174 , 269 ) | 244 ( 167 , 266 ) | 260 ( 165 , 274 ) |
| 2050s | 243 ( 170 , 264 ) | 258 ( 165 , 273 ) | 266 ( 163 , 278 ) | 277 ( 163 , 286 ) |
| 2060s | 246 ( 165 , 265 ) | 264 ( 163 , 277 ) | 277 ( 157 , 285 ) | 287 ( 267 , 293 ) |
| 2070s | 247 ( 166 , 267 ) | 273 ( 161 , 282 ) | 284 ( 253 , 290 ) | 291 ( 279 , 296 ) |
| 2080s | 243 ( 170 , 263 ) | 278 ( 160 , 286 ) | 289 ( 277 , 294 ) | 295 ( 286 , 300 ) |
| 2090s | 243 ( 169 , 264 ) | 280 ( 163 , 288 ) | 293 ( 282 , 298 ) | 298 ( 289 , 303 ) |

*The $day - of - year$ with minimum mortality estimates were identified from the fitted seasonal curve as the trough. The empirical confidence intervals (eCIs) for peak and trough were obtained through Monte Carlo simulations. These estimates are obtained by pooling location-specific estimates for each climate zone. We removed Feb 29 from the datasets and took values from 1 to 365 to represent the day-of-year, corresponding to 1 January through 31 December for locations in the northern hemisphere and 1 July to 30 June of the following year for locations in the southern hemisphere.

**Table S3**. Peak-to-trough ratio (95% confidence intervals) by decades for each climatic zone under scenarios

| Decades | SSP1-2.6 | SSP2-4.5 | SSP3-7.0 | SSP5-8.5 |
|---|---|---|---|---|
| Arid | | | | |
| 2000s | 1.19 ( 1.11 , 1.29 ) | 1.19 ( 1.11 , 1.29 ) | 1.19 ( 1.11 , 1.29 ) | 1.19 ( 1.11 , 1.29 ) |
| 2010s | 1.18 ( 1.1 , 1.27 ) | 1.18 ( 1.1 , 1.27 ) | 1.18 ( 1.1 , 1.27 ) | 1.18 ( 1.1 , 1.27 ) |
| 2020s | 1.17 ( 1.09 , 1.26 ) | 1.17 ( 1.09 , 1.26 ) | 1.18 ( 1.1 , 1.26 ) | 1.17 ( 1.09 , 1.26 ) |
| 2030s | 1.17 ( 1.09 , 1.25 ) | 1.17 ( 1.09 , 1.26 ) | 1.17 ( 1.09 , 1.25 ) | 1.17 ( 1.08 , 1.25 ) |
| 2040s | 1.17 ( 1.09 , 1.25 ) | 1.16 ( 1.08 , 1.25 ) | 1.16 ( 1.08 , 1.25 ) | 1.16 ( 1.08 , 1.24 ) |
| 2050s | 1.16 ( 1.08 , 1.25 ) | 1.16 ( 1.07 , 1.24 ) | 1.15 ( 1.07 , 1.24 ) | 1.15 ( 1.07 , 1.23 ) |
| 2060s | 1.16 ( 1.08 , 1.25 ) | 1.15 ( 1.07 , 1.24 ) | 1.15 ( 1.07 , 1.23 ) | 1.14 ( 1.06 , 1.23 ) |
| 2070s | 1.16 ( 1.08 , 1.25 ) | 1.15 ( 1.07 , 1.24 ) | 1.14 ( 1.06 , 1.23 ) | 1.14 ( 1.09 , 1.19 ) |
| 2080s | 1.16 ( 1.08 , 1.25 ) | 1.15 ( 1.07 , 1.23 ) | 1.14 ( 1.09 , 1.19 ) | 1.14 ( 1.09 , 1.19 ) |
| 2090s | 1.16 ( 1.08 , 1.25 ) | 1.14 ( 1.07 , 1.23 ) | 1.14 ( 1.09 , 1.19 ) | 1.14 ( 0.96 , 1.36 ) |
| Continental | | | | |
| 2000s | 1.21 ( 1.17 , 1.25 ) | 1.21 ( 1.17 , 1.25 ) | 1.21 ( 1.17 , 1.25 ) | 1.21 ( 1.17 , 1.25 ) |
| 2010s | 1.19 ( 1.16 , 1.22 ) | 1.2 ( 1.16 , 1.23 ) | 1.19 ( 1.16 , 1.22 ) | 1.19 ( 1.16 , 1.23 ) |
| 2020s | 1.18 ( 1.15 , 1.21 ) | 1.18 ( 1.16 , 1.21 ) | 1.18 ( 1.16 , 1.21 ) | 1.18 ( 1.16 , 1.21 ) |
| 2030s | 1.17 ( 1.15 , 1.2 ) | 1.17 ( 1.14 , 1.19 ) | 1.17 ( 1.15 , 1.2 ) | 1.17 ( 1.14 , 1.19 ) |
| 2040s | 1.17 ( 1.14 , 1.2 ) | 1.16 ( 1.14 , 1.19 ) | 1.16 ( 1.13 , 1.18 ) | 1.15 ( 1.13 , 1.18 ) |
| 2050s | 1.16 ( 1.14 , 1.18 ) | 1.15 ( 1.13 , 1.18 ) | 1.15 ( 1.12 , 1.17 ) | 1.14 ( 1.12 , 1.17 ) |
| 2060s | 1.16 ( 1.14 , 1.19 ) | 1.15 ( 1.12 , 1.18 ) | 1.14 ( 1.12 , 1.17 ) | 1.14 ( 1.11 , 1.17 ) |
| 2070s | 1.16 ( 1.13 , 1.19 ) | 1.15 ( 1.12 , 1.17 ) | 1.14 ( 1.11 , 1.17 ) | 1.15 ( 1.11 , 1.18 ) |
| 2080s | 1.16 ( 1.14 , 1.19 ) | 1.15 ( 1.12 , 1.17 ) | 1.14 ( 1.11 , 1.17 ) | 1.16 ( 1.06 , 1.27 ) |
| 2090s | 1.17 ( 1.14 , 1.19 ) | 1.14 ( 1.12 , 1.17 ) | 1.14 ( 1.11 , 1.17 ) | 1.22 ( 1.08 , 1.38 ) |
| Temperate | | | | |
| 2000s | 1.22 ( 1.18 , 1.26 ) | 1.22 ( 1.18 , 1.26 ) | 1.22 ( 1.18 , 1.26 ) | 1.22 ( 1.18 , 1.26 ) |
| 2010s | 1.21 ( 1.17 , 1.24 ) | 1.21 ( 1.17 , 1.25 ) | 1.21 ( 1.17 , 1.24 ) | 1.21 ( 1.17 , 1.25 ) |
| 2020s | 1.2 ( 1.17 , 1.24 ) | 1.2 ( 1.17 , 1.24 ) | 1.2 ( 1.17 , 1.24 ) | 1.21 ( 1.17 , 1.24 ) |
| 2030s | 1.2 ( 1.17 , 1.24 ) | 1.2 ( 1.16 , 1.23 ) | 1.2 ( 1.16 , 1.23 ) | 1.2 ( 1.16 , 1.23 ) |
| 2040s | 1.2 ( 1.16 , 1.23 ) | 1.2 ( 1.16 , 1.23 ) | 1.19 ( 1.16 , 1.22 ) | 1.19 ( 1.16 , 1.22 ) |
| 2050s | 1.19 ( 1.16 , 1.22 ) | 1.19 ( 1.16 , 1.22 ) | 1.18 ( 1.16 , 1.21 ) | 1.19 ( 1.16 , 1.22 ) |
| 2060s | 1.2 ( 1.16 , 1.23 ) | 1.19 ( 1.16 , 1.22 ) | 1.18 ( 1.16 , 1.21 ) | 1.18 ( 1.15 , 1.22 ) |
| 2070s | 1.19 ( 1.16 , 1.23 ) | 1.19 ( 1.16 , 1.22 ) | 1.18 ( 1.15 , 1.22 ) | 1.19 ( 1.16 , 1.22 ) |
| 2080s | 1.19 ( 1.16 , 1.23 ) | 1.19 ( 1.16 , 1.22 ) | 1.18 ( 1.15 , 1.21 ) | 1.22 ( 1.13 , 1.32 ) |
| 2090s | 1.2 ( 1.16 , 1.23 ) | 1.19 ( 1.15 , 1.22 ) | 1.19 ( 1.11 , 1.27 ) | 1.31 ( 1.18 , 1.44 ) |
| Tropical | | | | |
| 2000s | 1.04 ( 1 , 1.08 ) | 1.04 ( 1 , 1.08 ) | 1.04 ( 1 , 1.08 ) | 1.04 ( 1 , 1.08 ) |
| 2010s | 1.04 ( 1 , 1.07 ) | 1.03 ( 1 , 1.07 ) | 1.03 ( 1 , 1.07 ) | 1.04 ( 1 , 1.07 ) |

| | | | | |
|---|---|---|---|---|
| 2020s | 1.03 ( 0.99 , 1.06 ) | 1.03 ( 1 , 1.06 ) | 1.03 ( 1 , 1.06 ) | 1.03 ( 1 , 1.06 ) |
| 2030s | 1.02 ( 0.99 , 1.06 ) | 1.03 ( 0.99 , 1.07 ) | 1.03 ( 0.99 , 1.07 ) | 1.03 ( 0.99 , 1.08 ) |
| 2040s | 1.03 ( 0.97 , 1.09 ) | 1.03 ( 0.98 , 1.08 ) | 1.03 ( 0.98 , 1.09 ) | 1.04 ( 0.99 , 1.1 ) |
| 2050s | 1.03 ( 0.97 , 1.09 ) | 1.04 ( 0.99 , 1.09 ) | 1.04 ( 0.99 , 1.1 ) | 1.05 ( 1 , 1.11 ) |
| 2060s | 1.03 ( 0.97 , 1.09 ) | 1.05 ( 1 , 1.11 ) | 1.08 ( 1.02 , 1.14 ) | 1.11 ( 1.03 , 1.18 ) |
| 2070s | 1.02 ( 0.97 , 1.08 ) | 1.06 ( 1 , 1.12 ) | 1.12 ( 1.06 , 1.19 ) | 1.12 ( 1.03 , 1.22 ) |
| 2080s | 1.03 ( 0.98 , 1.08 ) | 1.06 ( 1 , 1.12 ) | 1.13 ( 1.04 , 1.23 ) | 1.14 ( 1.04 , 1.24 ) |
| 2090s | 1.02 ( 0.97 , 1.08 ) | 1.08 ( 1.02 , 1.14 ) | 1.15 ( 1.04 , 1.26 ) | 1.16 ( 1.05 , 1.27 ) |

The peak-to-trough ratio is the ratio of the maximum mortality estimate at peak day to the minimum mortality estimate at trough day. These estimates are obtained by pooling location-specific estimates for each climate zone. We removed Feb 29 from the datasets and took values from 1 to 365 to represent the day of year, corresponding to 1 January through 31 December for locations in the northern hemisphere and 1 July to 30 June of the following year for locations in the southern hemisphere.

**Table S4**. Attributable fraction (95% empirical confidence intervals) by decades for each climatic zone under scenarios

| Period | SSP1-2.6 | SSP2-4.5 | SSP3-7.0 | SSP5-8.5 |
|---|---|---|---|---|
| Arid | | | | |
| 2000s | 0.06 ( 0.04 , 0.09 ) | 0.06 ( 0.04 , 0.09 ) | 0.06 ( 0.04 , 0.09 ) | 0.06 ( 0.04 , 0.09 ) |
| 2010s | 0.05 ( 0.04 , 0.09 ) | 0.05 ( 0.04 , 0.09 ) | 0.05 ( 0.04 , 0.09 ) | 0.05 ( 0.04 , 0.08 ) |
| 2020s | 0.05 ( 0.03 , 0.08 ) | 0.05 ( 0.03 , 0.08 ) | 0.05 ( 0.04 , 0.08 ) | 0.05 ( 0.03 , 0.08 ) |
| 2030s | 0.05 ( 0.03 , 0.08 ) | 0.05 ( 0.03 , 0.08 ) | 0.05 ( 0.03 , 0.08 ) | 0.05 ( 0.03 , 0.08 ) |
| 2040s | 0.05 ( 0.03 , 0.08 ) | 0.04 ( 0.03 , 0.08 ) | 0.04 ( 0.03 , 0.08 ) | 0.04 ( 0.03 , 0.08 ) |
| 2050s | 0.04 ( 0.03 , 0.08 ) | 0.04 ( 0.03 , 0.08 ) | 0.04 ( 0.03 , 0.08 ) | 0.04 ( 0.03 , 0.08 ) |
| 2060s | 0.04 ( 0.03 , 0.08 ) | 0.04 ( 0.03 , 0.08 ) | 0.04 ( 0.03 , 0.08 ) | 0.04 ( 0.03 , 0.09 ) |
| 2070s | 0.04 ( 0.03 , 0.08 ) | 0.04 ( 0.03 , 0.08 ) | 0.04 ( 0.03 , 0.09 ) | 0.05 ( 0.03 , 0.09 ) |
| 2080s | 0.04 ( 0.03 , 0.08 ) | 0.04 ( 0.03 , 0.08 ) | 0.04 ( 0.03 , 0.09 ) | 0.05 ( 0.03 , 0.1 ) |
| 2090s | 0.05 ( 0.03 , 0.08 ) | 0.04 ( 0.03 , 0.08 ) | 0.05 ( 0.03 , 0.1 ) | 0.06 ( 0.03 , 0.11 ) |
| Continental | | | | |
| 2000s | 0.08 ( 0.06 , 0.09 ) | 0.08 ( 0.06 , 0.09 ) | 0.08 ( 0.06 , 0.09 ) | 0.08 ( 0.06 , 0.09 ) |
| 2010s | 0.07 ( 0.06 , 0.08 ) | 0.07 ( 0.06 , 0.08 ) | 0.07 ( 0.06 , 0.08 ) | 0.07 ( 0.06 , 0.08 ) |
| 2020s | 0.07 ( 0.06 , 0.08 ) | 0.07 ( 0.06 , 0.08 ) | 0.06 ( 0.06 , 0.08 ) | 0.06 ( 0.06 , 0.08 ) |
| 2030s | 0.06 ( 0.05 , 0.07 ) | 0.06 ( 0.05 , 0.07 ) | 0.06 ( 0.05 , 0.07 ) | 0.05 ( 0.05 , 0.07 ) |
| 2040s | 0.05 ( 0.05 , 0.07 ) | 0.05 ( 0.05 , 0.06 ) | 0.05 ( 0.04 , 0.07 ) | 0.05 ( 0.04 , 0.06 ) |
| 2050s | 0.05 ( 0.05 , 0.06 ) | 0.05 ( 0.04 , 0.06 ) | 0.05 ( 0.04 , 0.06 ) | 0.05 ( 0.04 , 0.06 ) |
| 2060s | 0.05 ( 0.05 , 0.06 ) | 0.05 ( 0.04 , 0.06 ) | 0.05 ( 0.04 , 0.06 ) | 0.05 ( 0.04 , 0.07 ) |
| 2070s | 0.05 ( 0.04 , 0.07 ) | 0.05 ( 0.04 , 0.06 ) | 0.05 ( 0.04 , 0.07 ) | 0.06 ( 0.04 , 0.09 ) |
| 2080s | 0.05 ( 0.05 , 0.07 ) | 0.05 ( 0.04 , 0.06 ) | 0.06 ( 0.04 , 0.08 ) | 0.08 ( 0.05 , 0.1 ) |
| 2090s | 0.05 ( 0.05 , 0.07 ) | 0.05 ( 0.04 , 0.06 ) | 0.07 ( 0.05 , 0.09 ) | 0.09 ( 0.05 , 0.12 ) |
| Temperate | | | | |
| 2000s | 0.07 ( 0.06 , 0.08 ) | 0.07 ( 0.06 , 0.08 ) | 0.07 ( 0.06 , 0.08 ) | 0.07 ( 0.06 , 0.08 ) |
| 2010s | 0.06 ( 0.05 , 0.07 ) | 0.06 ( 0.05 , 0.07 ) | 0.06 ( 0.05 , 0.07 ) | 0.06 ( 0.05 , 0.07 ) |
| 2020s | 0.06 ( 0.05 , 0.07 ) | 0.06 ( 0.05 , 0.07 ) | 0.06 ( 0.05 , 0.07 ) | 0.06 ( 0.05 , 0.07 ) |
| 2030s | 0.06 ( 0.05 , 0.07 ) | 0.06 ( 0.05 , 0.07 ) | 0.06 ( 0.05 , 0.07 ) | 0.06 ( 0.05 , 0.07 ) |
| 2040s | 0.06 ( 0.05 , 0.07 ) | 0.06 ( 0.05 , 0.07 ) | 0.06 ( 0.05 , 0.07 ) | 0.06 ( 0.05 , 0.07 ) |
| 2050s | 0.06 ( 0.05 , 0.07 ) | 0.06 ( 0.05 , 0.07 ) | 0.06 ( 0.05 , 0.07 ) | 0.07 ( 0.05 , 0.08 ) |
| 2060s | 0.06 ( 0.05 , 0.07 ) | 0.06 ( 0.05 , 0.07 ) | 0.07 ( 0.05 , 0.08 ) | 0.07 ( 0.06 , 0.09 ) |
| 2070s | 0.06 ( 0.05 , 0.07 ) | 0.06 ( 0.05 , 0.08 ) | 0.07 ( 0.06 , 0.08 ) | 0.08 ( 0.06 , 0.1 ) |
| 2080s | 0.06 ( 0.05 , 0.07 ) | 0.07 ( 0.05 , 0.08 ) | 0.08 ( 0.06 , 0.09 ) | 0.09 ( 0.07 , 0.11 ) |
| 2090s | 0.06 ( 0.05 , 0.07 ) | 0.07 ( 0.05 , 0.08 ) | 0.08 ( 0.06 , 0.1 ) | 0.11 ( 0.08 , 0.14 ) |
| Tropical | | | | |
| 2000s | 0.02 ( 0.01 , 0.04 ) | 0.02 ( 0.01 , 0.04 ) | 0.02 ( 0.01 , 0.04 ) | 0.02 ( 0.01 , 0.04 ) |
| 2010s | 0.02 ( 0.01 , 0.04 ) | 0.02 ( 0.01 , 0.04 ) | 0.02 ( 0.01 , 0.04 ) | 0.02 ( 0.01 , 0.04 ) |

| | | | | |
|---|---|---|---|---|
| 2020s | 0.01 ( 0.01 , 0.04 ) | 0.01 ( 0.01 , 0.04 ) | 0.02 ( 0.01 , 0.04 ) | 0.02 ( 0.01 , 0.04 ) |
| 2030s | 0.01 ( 0.01 , 0.04 ) | 0.01 ( 0.01 , 0.04 ) | 0.01 ( 0.01 , 0.04 ) | 0.01 ( 0.01 , 0.04 ) |
| 2040s | 0.01 ( 0.01 , 0.04 ) | 0.01 ( 0.01 , 0.04 ) | 0.01 ( 0.01 , 0.05 ) | 0.02 ( 0.01 , 0.05 ) |
| 2050s | 0.01 ( 0.01 , 0.04 ) | 0.02 ( 0.01 , 0.05 ) | 0.02 ( 0.01 , 0.05 ) | 0.03 ( 0.01 , 0.06 ) |
| 2060s | 0.01 ( 0.01 , 0.04 ) | 0.02 ( 0.01 , 0.05 ) | 0.04 ( 0.02 , 0.07 ) | 0.05 ( 0.03 , 0.09 ) |
| 2070s | 0.01 ( 0.01 , 0.04 ) | 0.03 ( 0.01 , 0.06 ) | 0.06 ( 0.04 , 0.09 ) | 0.06 ( 0.03 , 0.11 ) |
| 2080s | 0.01 ( 0.01 , 0.04 ) | 0.03 ( 0.01 , 0.07 ) | 0.06 ( 0.03 , 0.11 ) | 0.07 ( 0.03 , 0.12 ) |
| 2090s | 0.01 ( 0.01 , 0.04 ) | 0.04 ( 0.02 , 0.07 ) | 0.07 ( 0.03 , 0.12 ) | 0.08 ( 0.04 , 0.15 ) |

The attributable fraction estimates the fraction by which mortality would be reduced in a counterfactual scenario where mortality risk never rose above its seasonal trough. These estimates are obtained by pooling location-specific estimates for each climate zone. We removed Feb 29 from the datasets and took values from 1 to 365 to represent the day of year, corresponding to 1 January through 31 December for locations in the northern hemisphere and 1 July to 30 June of the following year for locations in the southern hemisphere.

**Figure S1.** Shape of seasonality of mortality in each country/area from the 2000s to 2090s under four scenarios

The seasonality is computed as the relative risk of mortality estimates at each day-of-year *i* to minimum mortality estimates at the trough day for each country/ area:

$$\text{Relative risk}=\text{Mortality estimate at day}-\text{of}-\text{year}_i/\text{Minimum mortality estimate at the trough}$$

These estimates are obtained by pooling location-specific estimates for each country/area. We removed Feb 29 from the datasets. When reporting results at the country/area level, we took values from 1 to 365 to represent the day-of-year, corresponding to 1 January through 31 December for locations in both hemispheres. Note that the scales are different in each row, as the relative risk varies substantially between countries.

**Note:** The two polar locations in Peru were included when pooling the results for Peru.

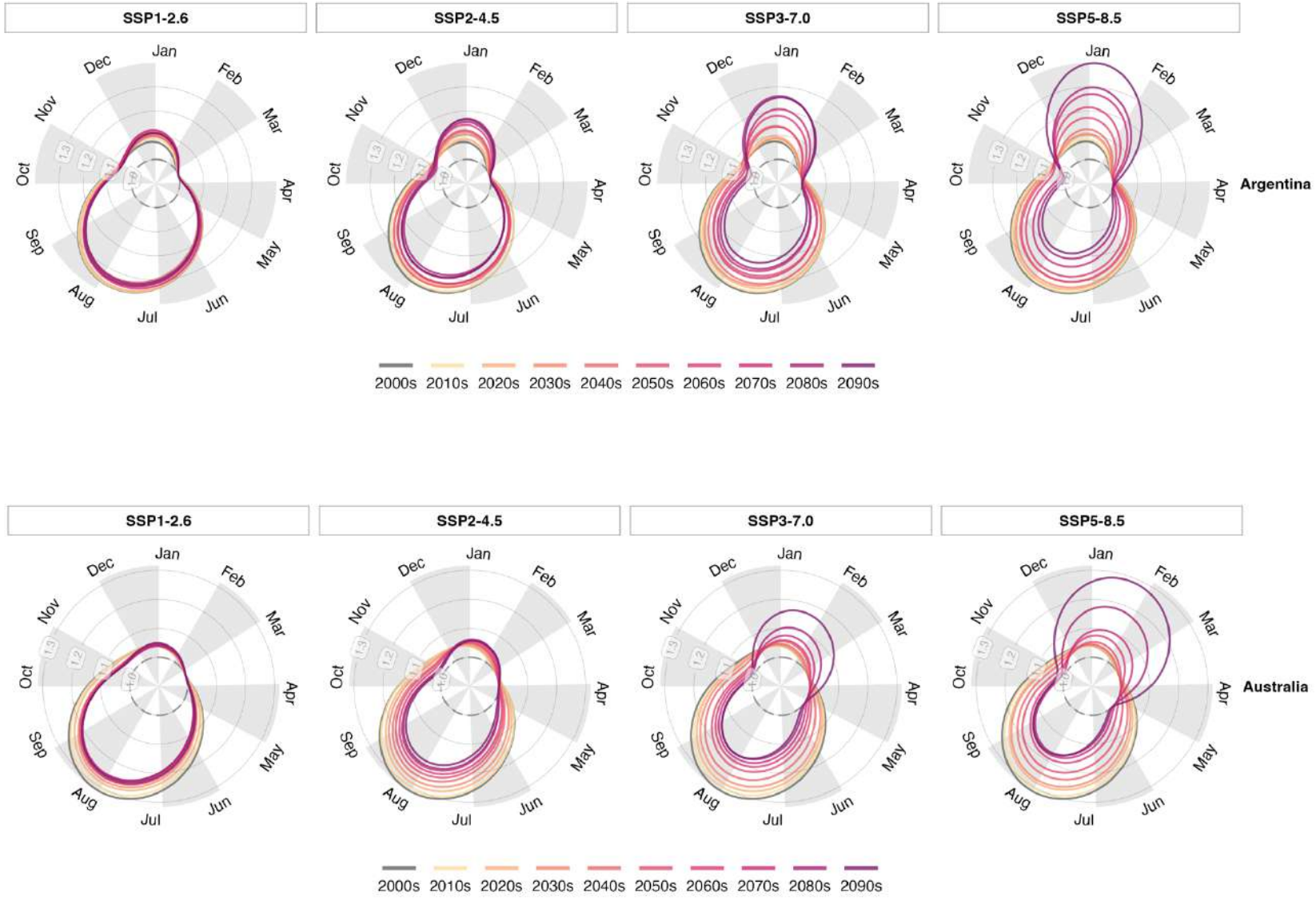
SSP1-2.6
SSP2-4.5
SSP3-7.0
SSP5-8.5
Jan
Feb
Mar
Apr
May
Jun
Jul
Aug
Sep
Oct
Nov
Dec
Argentina
Australia
2000s
2010s
2020s
2030s
2040s
2050s
2060s
2070s
2080s
2090s

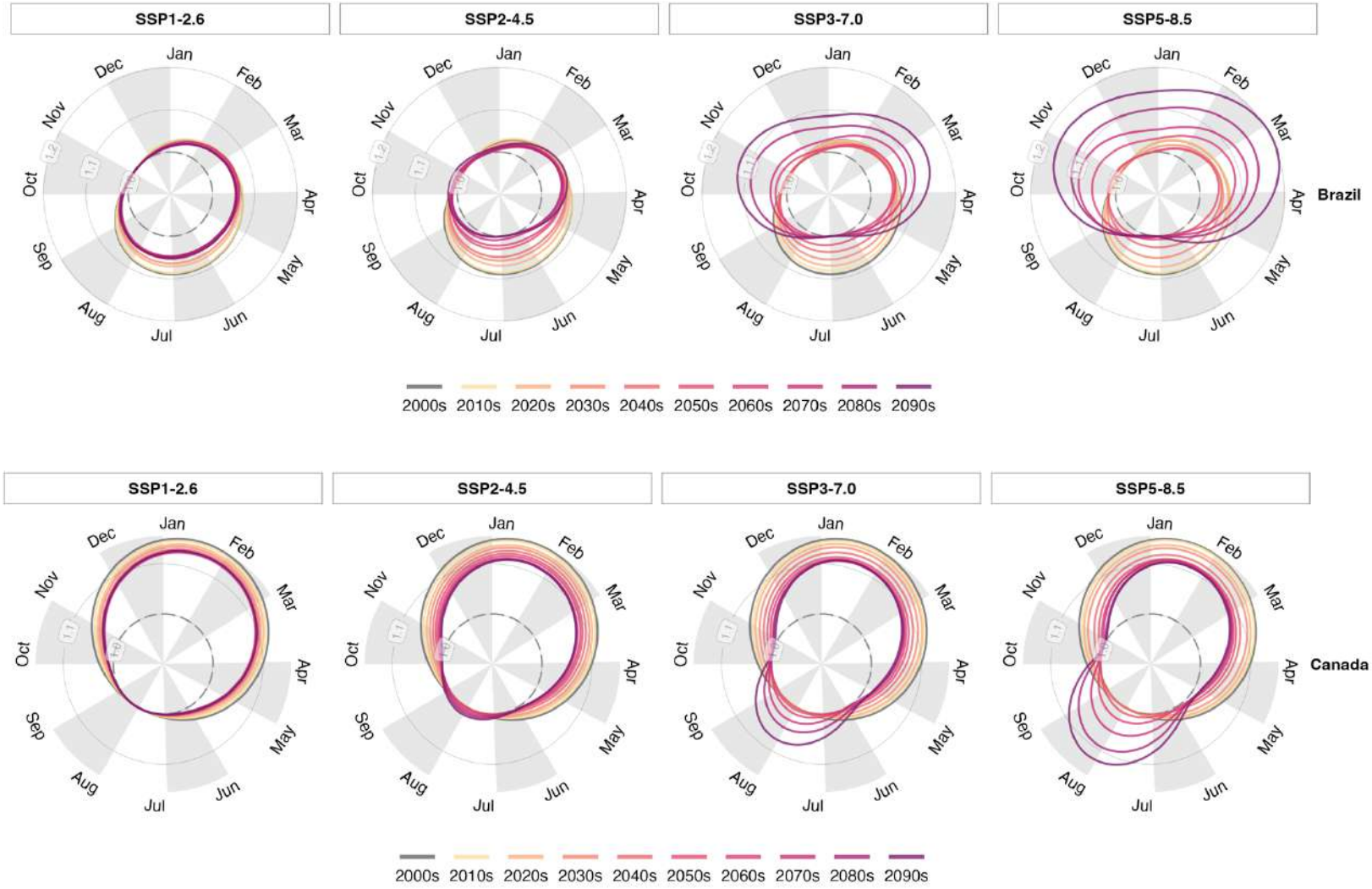
SSP1-2.6
SSP2-4.5
SSP3-7.0
SSP5-8.5
Jan
Feb
Mar
Apr
May
Jun
Jul
Aug
Sep
Oct
Nov
Dec
Brazil
2000s 2010s 2020s 2030s 2040s 2050s 2060s 2070s 2080s 2090s
SSP1-2.6
SSP2-4.5
SSP3-7.0
SSP5-8.5
Canada
2000s 2010s 2020s 2030s 2040s 2050s 2060s 2070s 2080s 2090s

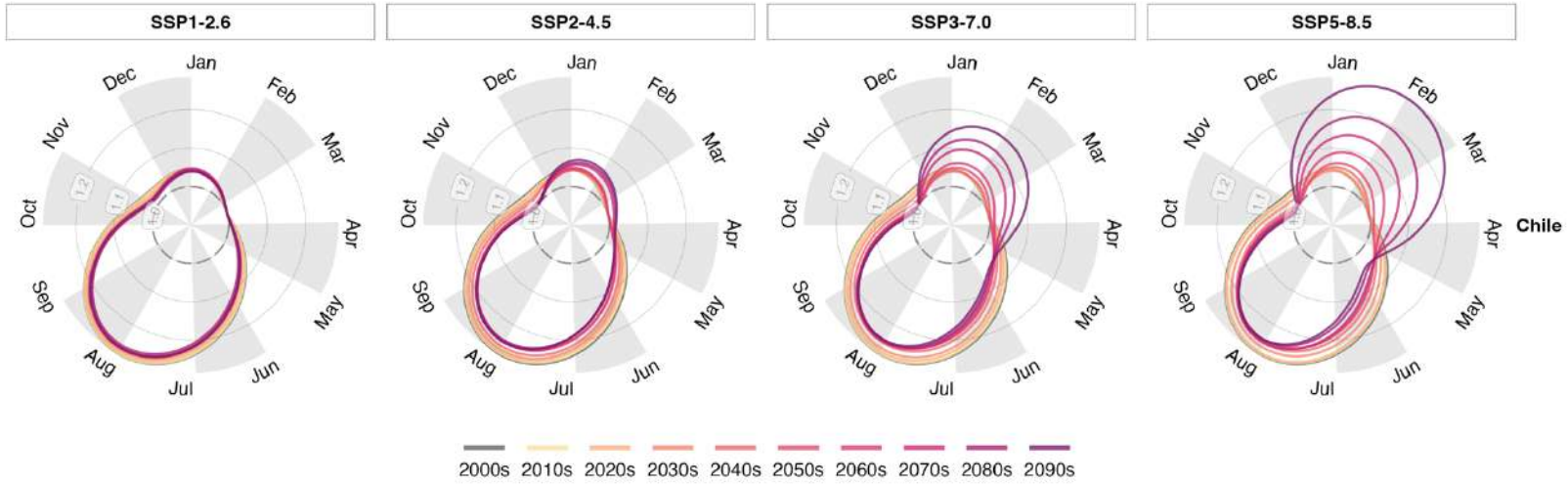
SSP1-2.6
SSP2-4.5
SSP3-7.0
SSP5-8.5
Jan
Feb
Mar
Apr
May
Jun
Jul
Aug
Sep
Oct
Nov
Dec
Chile
2000s
2010s
2020s
2030s
2040s
2050s
2060s
2070s
2080s
2090s

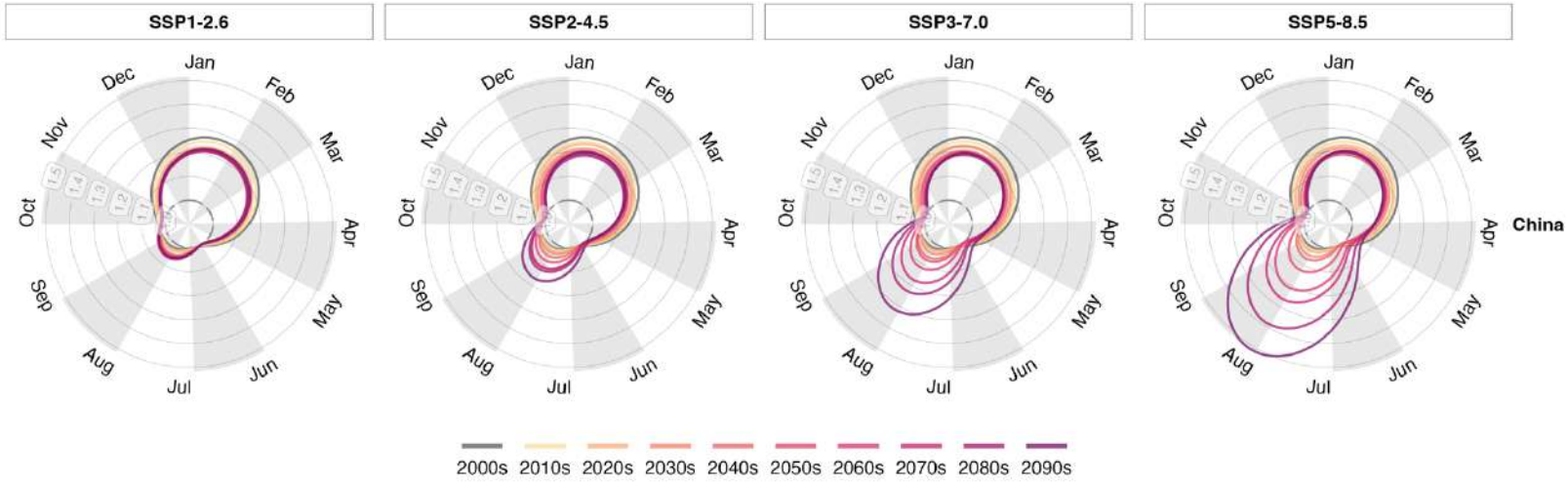
SSP1-2.6
SSP2-4.5
SSP3-7.0
SSP5-8.5
Jan
Feb
Mar
Apr
May
Jun
Jul
Aug
Sep
Oct
Nov
Dec
China
2000s
2010s
2020s
2030s
2040s
2050s
2060s
2070s
2080s
2090s

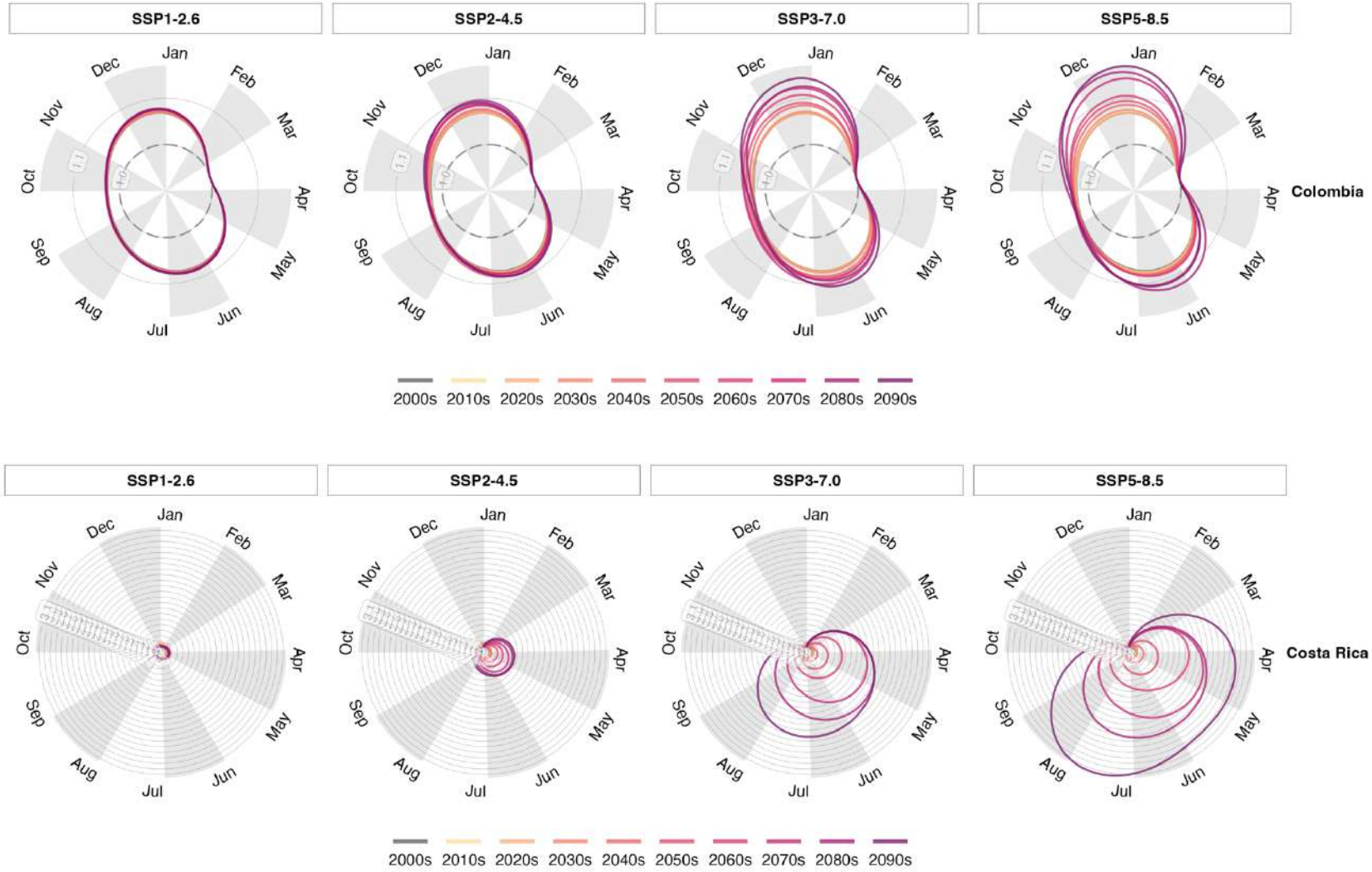
SSP1-2.6
SSP2-4.5
SSP3-7.0
SSP5-8.5
Jan
Feb
Mar
Apr
May
Jun
Jul
Aug
Sep
Oct
Nov
Dec
Colombia
2000s 2010s 2020s 2030s 2040s 2050s 2060s 2070s 2080s 2090s
SSP1-2.6
SSP2-4.5
SSP3-7.0
SSP5-8.5
Costa Rica
2000s 2010s 2020s 2030s 2040s 2050s 2060s 2070s 2080s 2090s

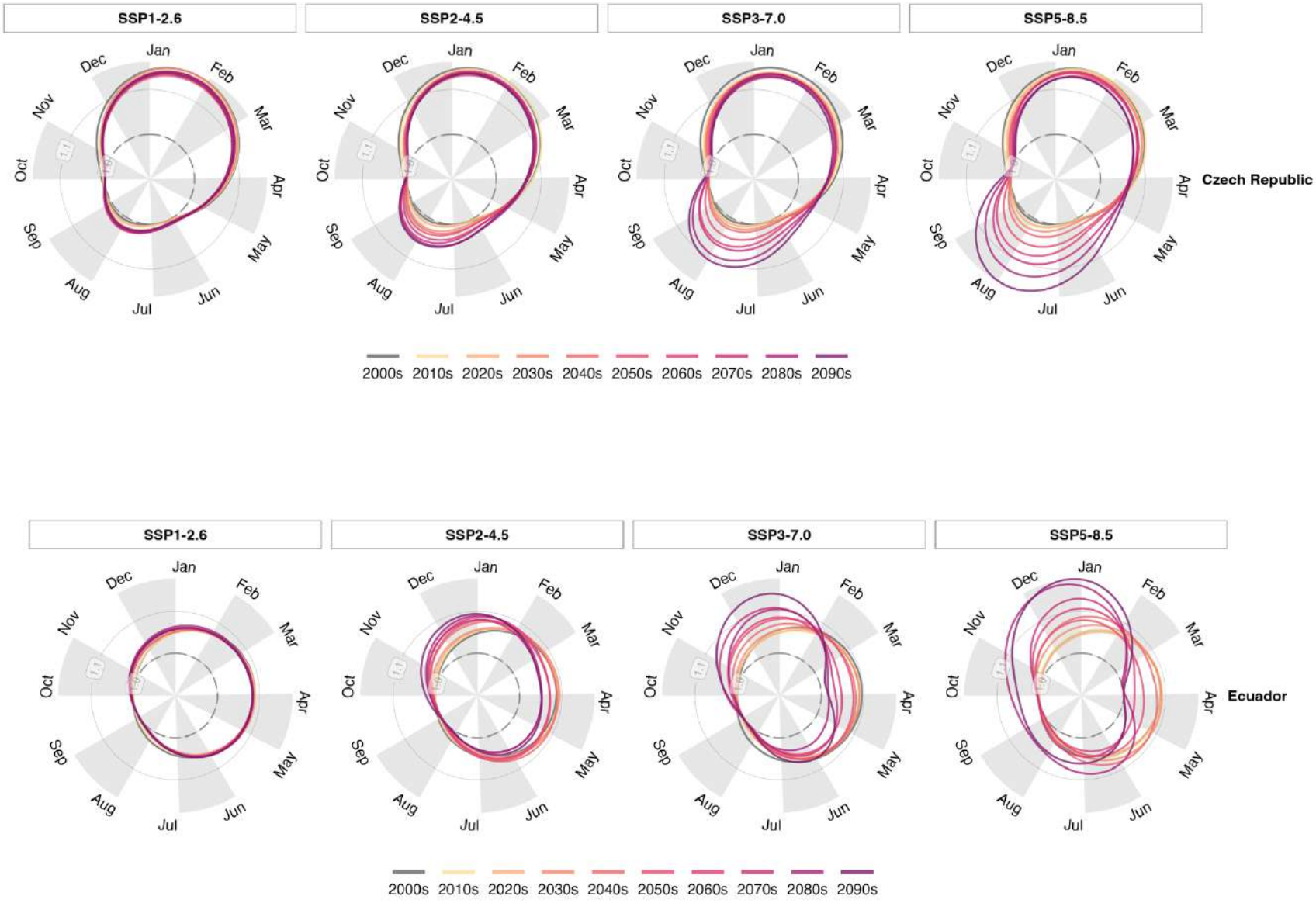
SSP1-2.6
SSP2-4.5
SSP3-7.0
SSP5-8.5
Jan
Feb
Mar
Apr
May
Jun
Jul
Aug
Sep
Oct
Nov
Dec
Czech Republic
Ecuador
2000s
2010s
2020s
2030s
2040s
2050s
2060s
2070s
2080s
2090s

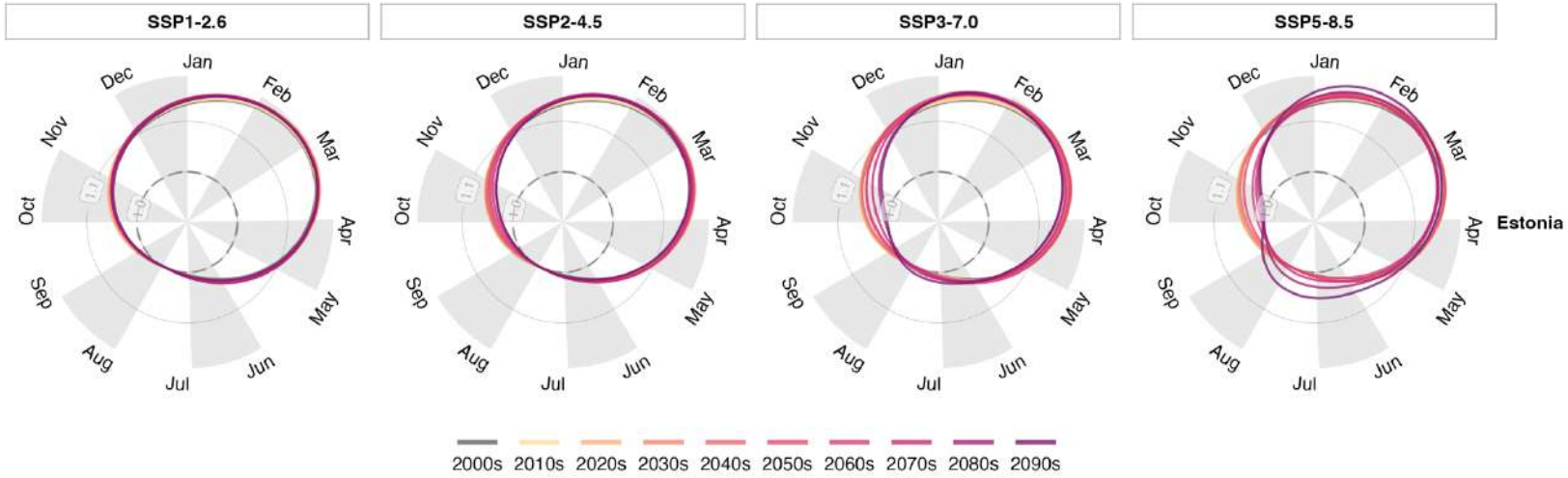
SSP1-2.6
SSP2-4.5
SSP3-7.0
SSP5-8.5
Jan
Feb
Mar
Apr
May
Jun
Jul
Aug
Sep
Oct
Nov
Dec
Estonia
2000s 2010s 2020s 2030s 2040s 2050s 2060s 2070s 2080s 2090s

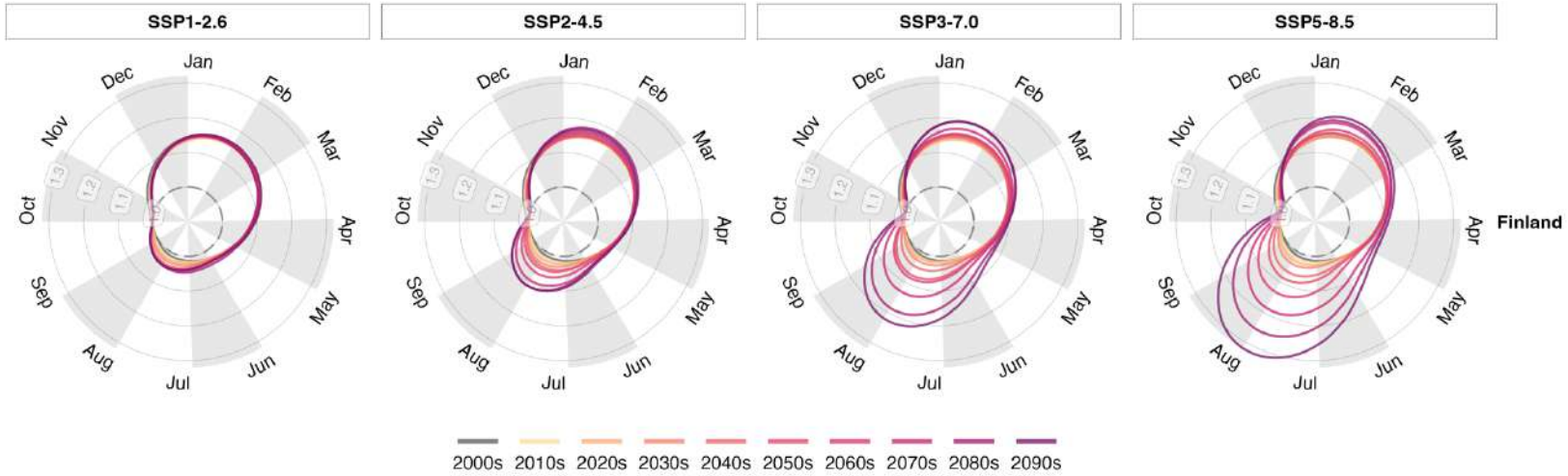
SSP1-2.6
SSP2-4.5
SSP3-7.0
SSP5-8.5
Jan
Feb
Mar
Apr
May
Jun
Jul
Aug
Sep
Oct
Nov
Dec
Finland
2000s 2010s 2020s 2030s 2040s 2050s 2060s 2070s 2080s 2090s

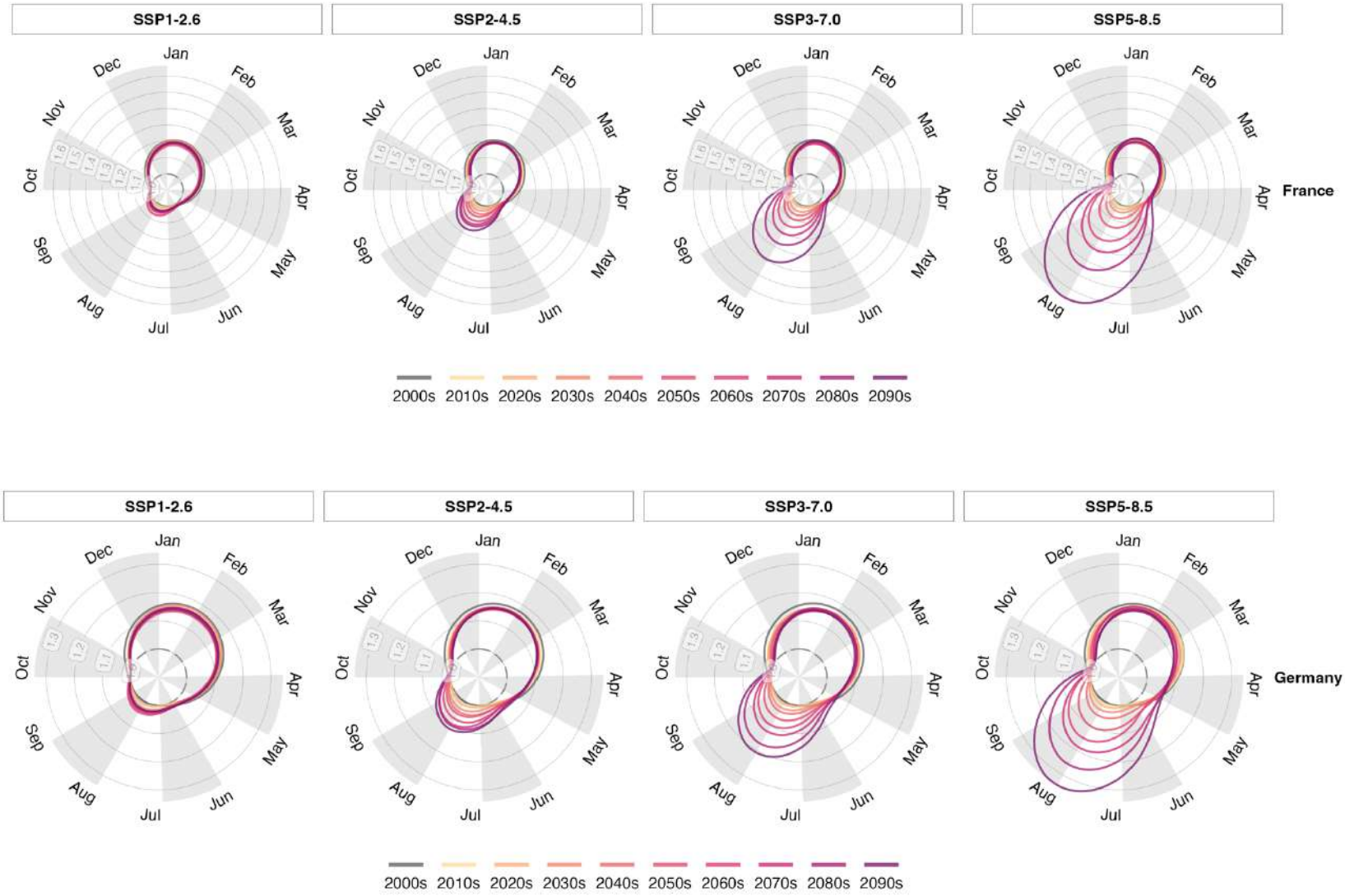
SSP1-2.6
SSP2-4.5
SSP3-7.0
SSP5-8.5
Jan
Feb
Mar
Apr
May
Jun
Jul
Aug
Sep
Oct
Nov
Dec
France
Germany
2000s
2010s
2020s
2030s
2040s
2050s
2060s
2070s
2080s
2090s

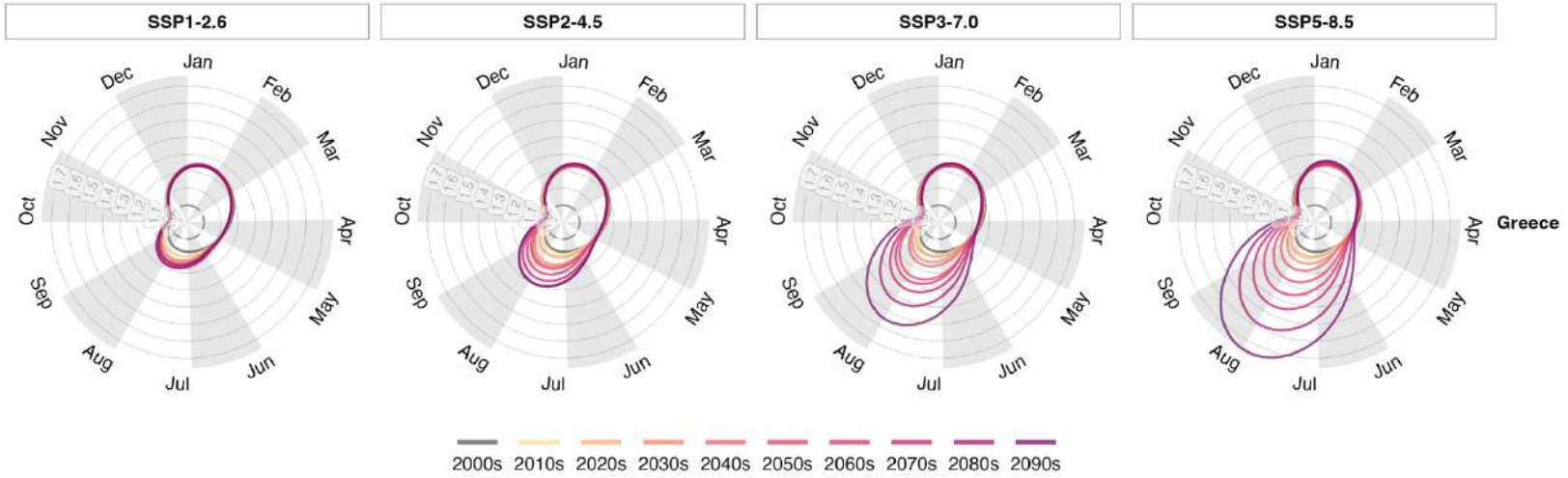
SSP1-2.6
SSP2-4.5
SSP3-7.0
SSP5-8.5
Jan
Feb
Mar
Apr
May
Jun
Jul
Aug
Sep
Oct
Nov
Dec
Greece
2000s
2010s
2020s
2030s
2040s
2050s
2060s
2070s
2080s
2090s

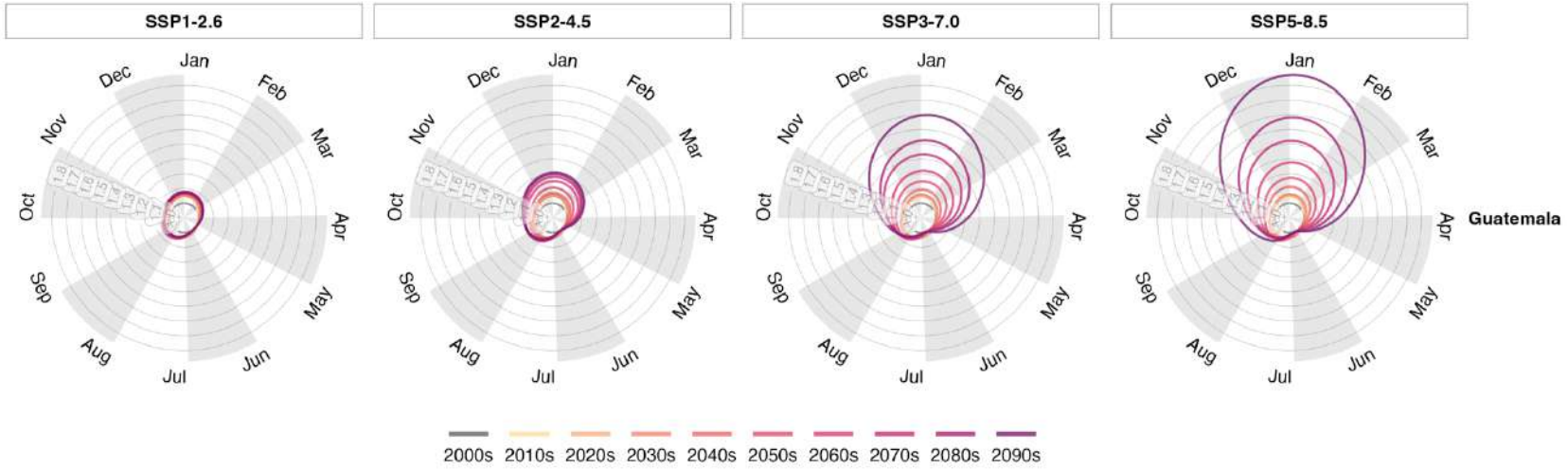
SSP1-2.6
SSP2-4.5
SSP3-7.0
SSP5-8.5
Jan
Feb
Mar
Apr
May
Jun
Jul
Aug
Sep
Oct
Nov
Dec
Guatemala
2000s
2010s
2020s
2030s
2040s
2050s
2060s
2070s
2080s
2090s

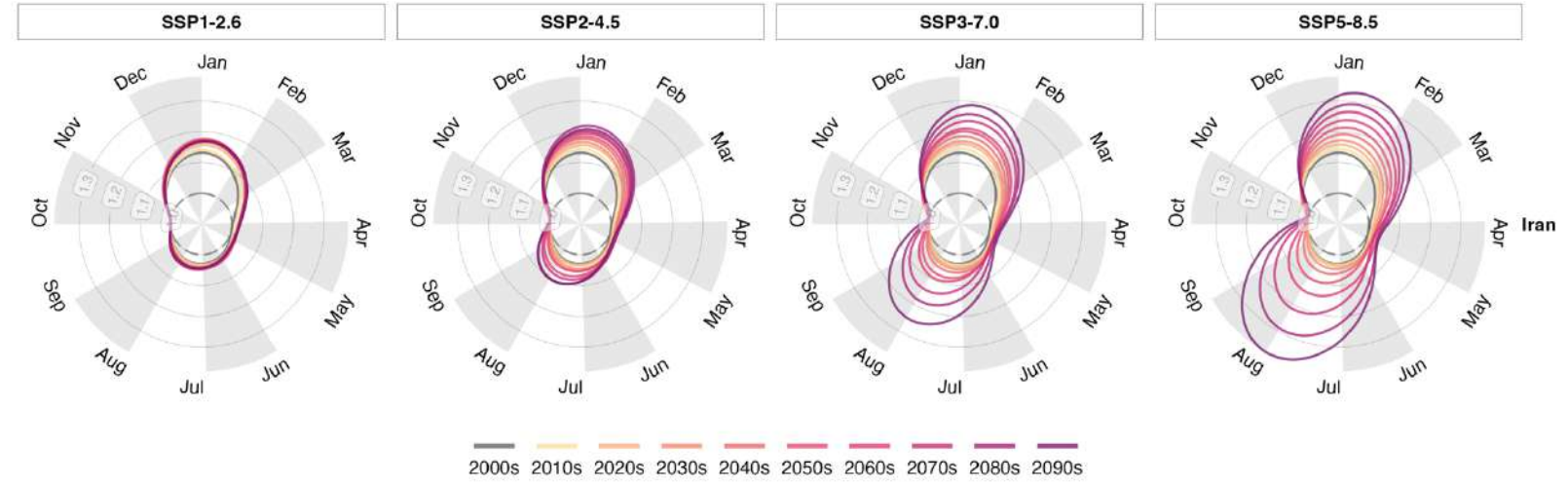
SSP1-2.6
SSP2-4.5
SSP3-7.0
SSP5-8.5
Jan
Feb
Mar
Apr
May
Jun
Jul
Aug
Sep
Oct
Nov
Dec
Iran
2000s 2010s 2020s 2030s 2040s 2050s 2060s 2070s 2080s 2090s

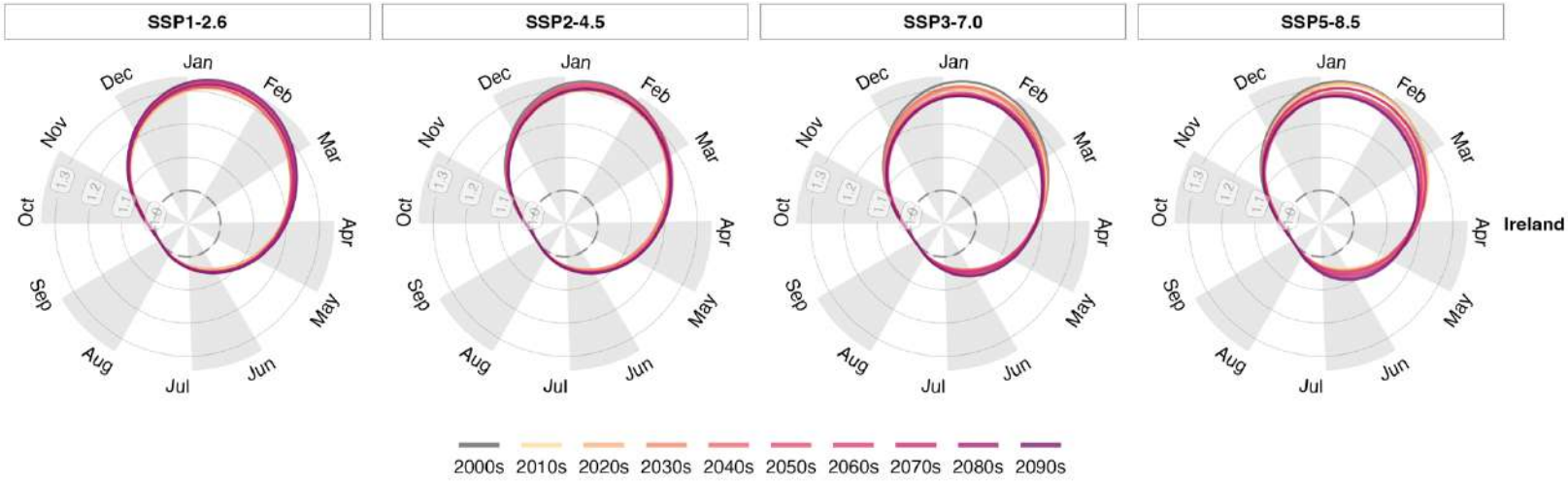
SSP1-2.6
SSP2-4.5
SSP3-7.0
SSP5-8.5
Jan
Feb
Mar
Apr
May
Jun
Jul
Aug
Sep
Oct
Nov
Dec
Ireland
2000s 2010s 2020s 2030s 2040s 2050s 2060s 2070s 2080s 2090s

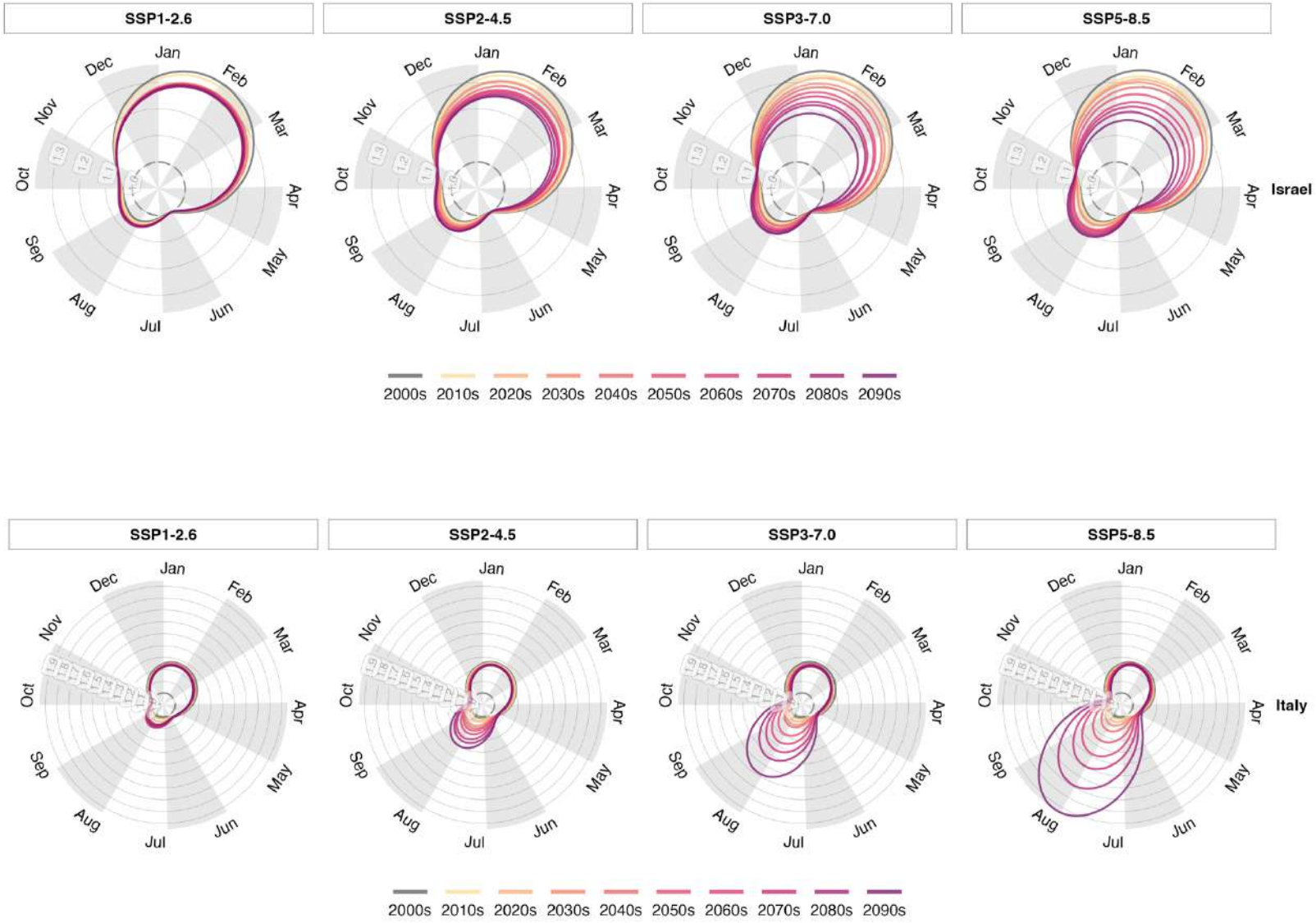
SSP1-2.6
SSP2-4.5
SSP3-7.0
SSP5-8.5
Israel
Italy
Jan
Feb
Mar
Apr
May
Jun
Jul
Aug
Sep
Oct
Nov
Dec
2000s
2010s
2020s
2030s
2040s
2050s
2060s
2070s
2080s
2090s

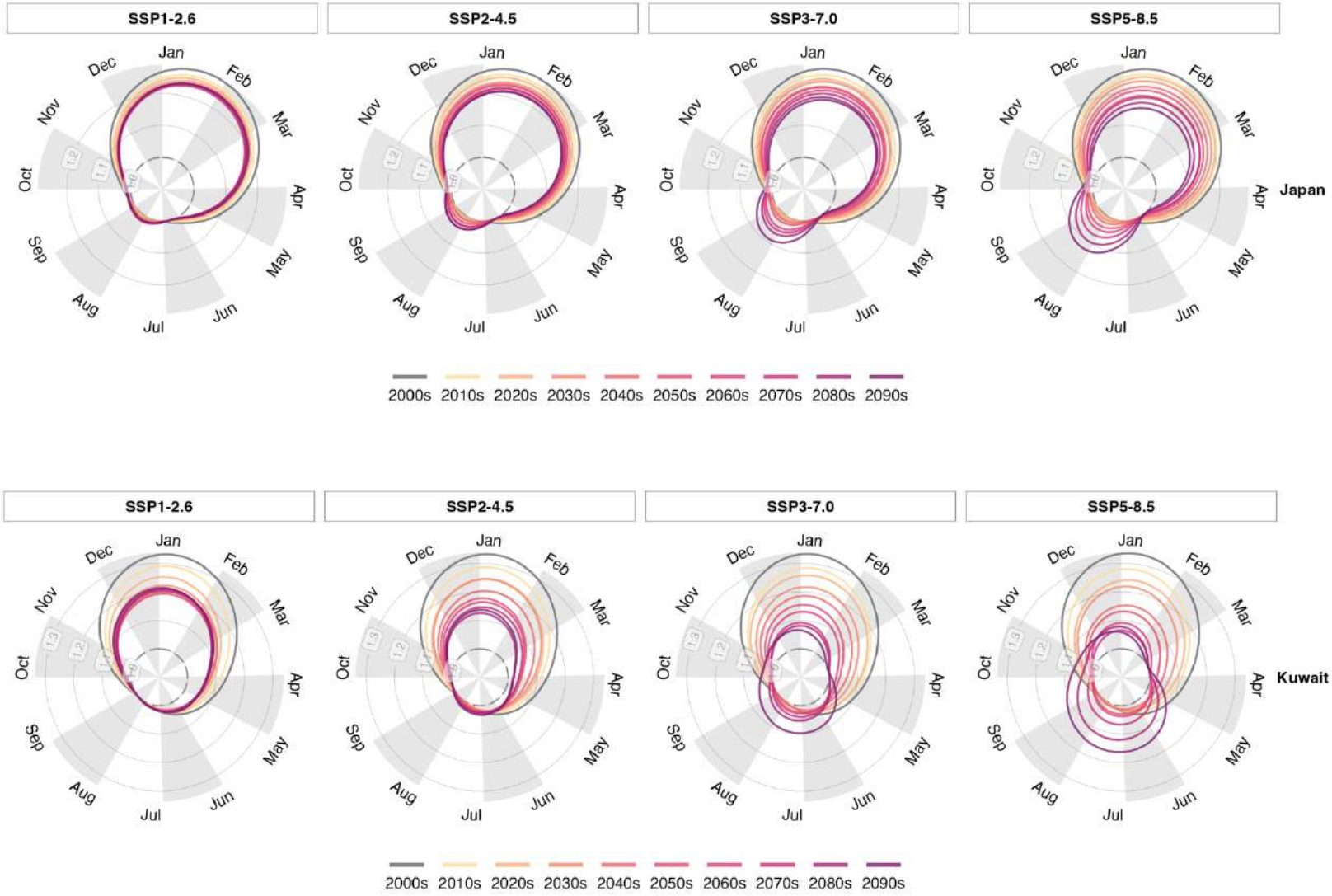
SSP1-2.6
SSP2-4.5
SSP3-7.0
SSP5-8.5
Jan
Feb
Mar
Apr
May
Jun
Jul
Aug
Sep
Oct
Nov
Dec
Japan
Kuwait
2000s
2010s
2020s
2030s
2040s
2050s
2060s
2070s
2080s
2090s

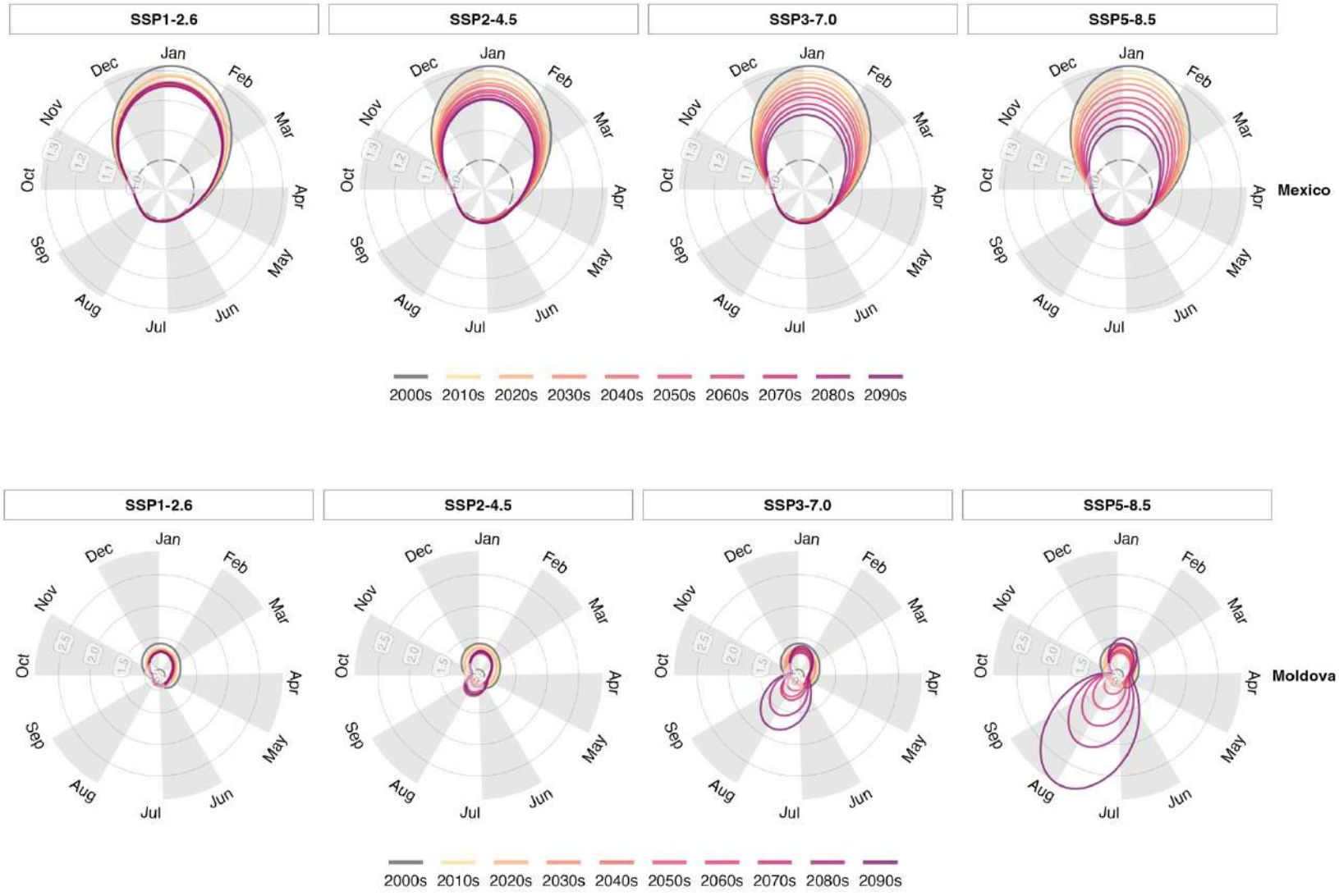
SSP1-2.6
SSP2-4.5
SSP3-7.0
SSP5-8.5
Jan
Feb
Mar
Apr
May
Jun
Jul
Aug
Sep
Oct
Nov
Dec
Mexico
Moldova
2000s
2010s
2020s
2030s
2040s
2050s
2060s
2070s
2080s
2090s

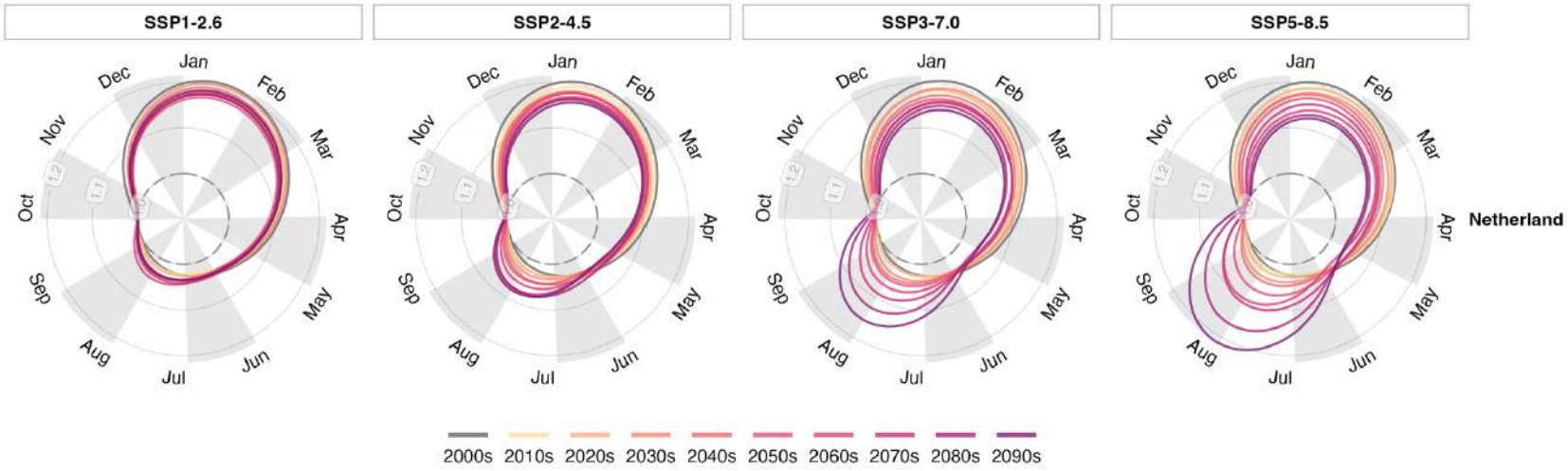
SSP1-2.6
SSP2-4.5
SSP3-7.0
SSP5-8.5
Jan
Feb
Mar
Apr
May
Jun
Jul
Aug
Sep
Oct
Nov
Dec
1.2
1.1
1.0
Netherland
2000s
2010s
2020s
2030s
2040s
2050s
2060s
2070s
2080s
2090s

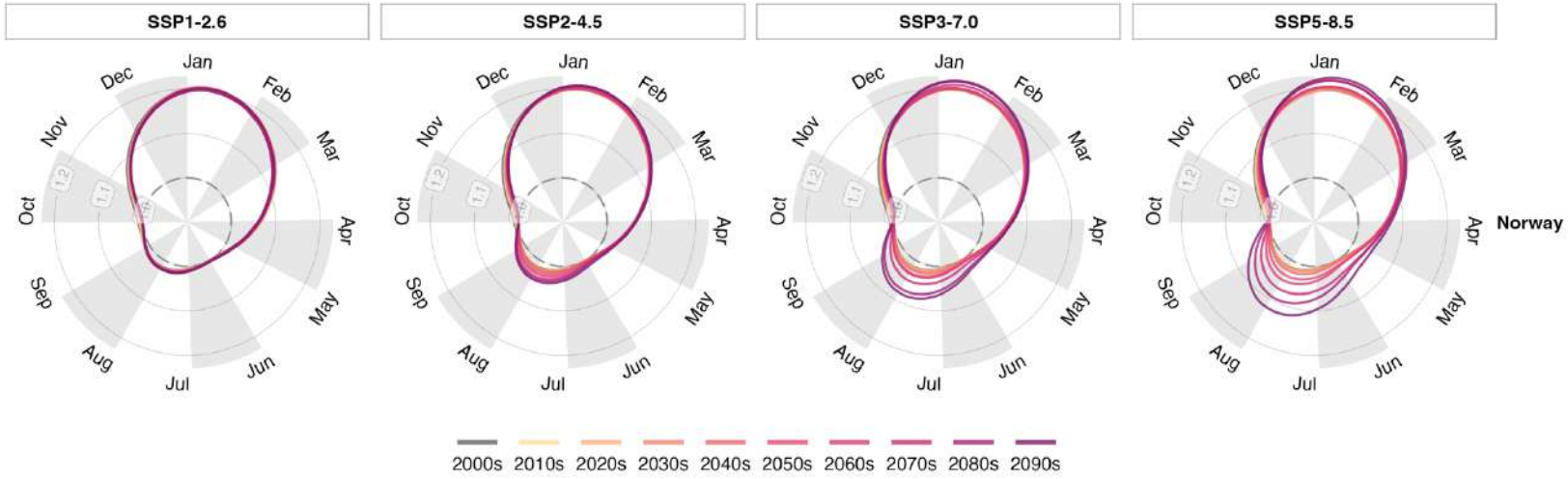
SSP1-2.6
SSP2-4.5
SSP3-7.0
SSP5-8.5
Jan
Feb
Mar
Apr
May
Jun
Jul
Aug
Sep
Oct
Nov
Dec
1.2
1.1
1.0
Norway
2000s
2010s
2020s
2030s
2040s
2050s
2060s
2070s
2080s
2090s

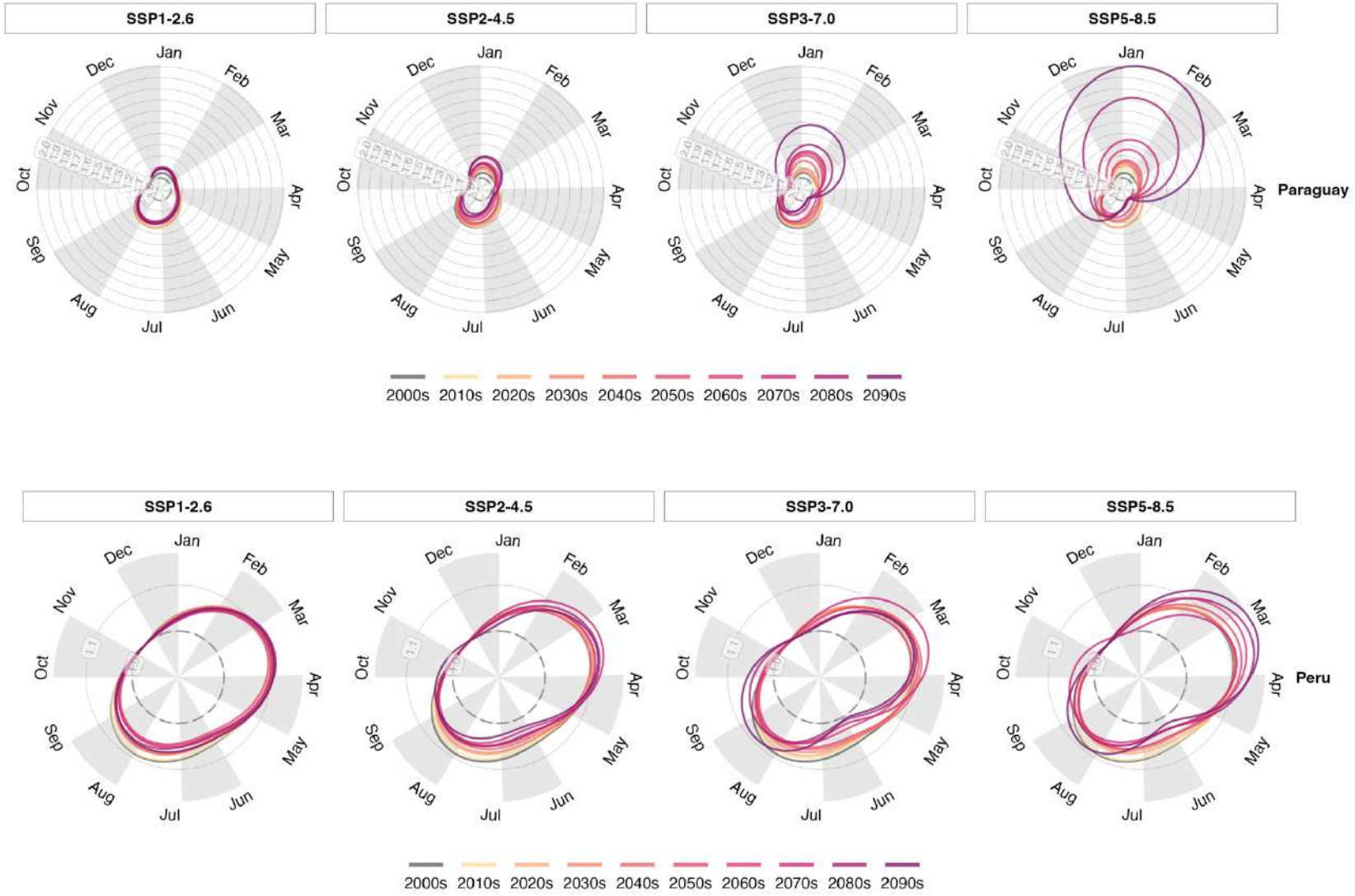
SSP1-2.6
SSP2-4.5
SSP3-7.0
SSP5-8.5
Jan
Feb
Mar
Apr
May
Jun
Jul
Aug
Sep
Oct
Nov
Dec
Paraguay
2000s 2010s 2020s 2030s 2040s 2050s 2060s 2070s 2080s 2090s
SSP1-2.6
SSP2-4.5
SSP3-7.0
SSP5-8.5
Peru
2000s 2010s 2020s 2030s 2040s 2050s 2060s 2070s 2080s 2090s

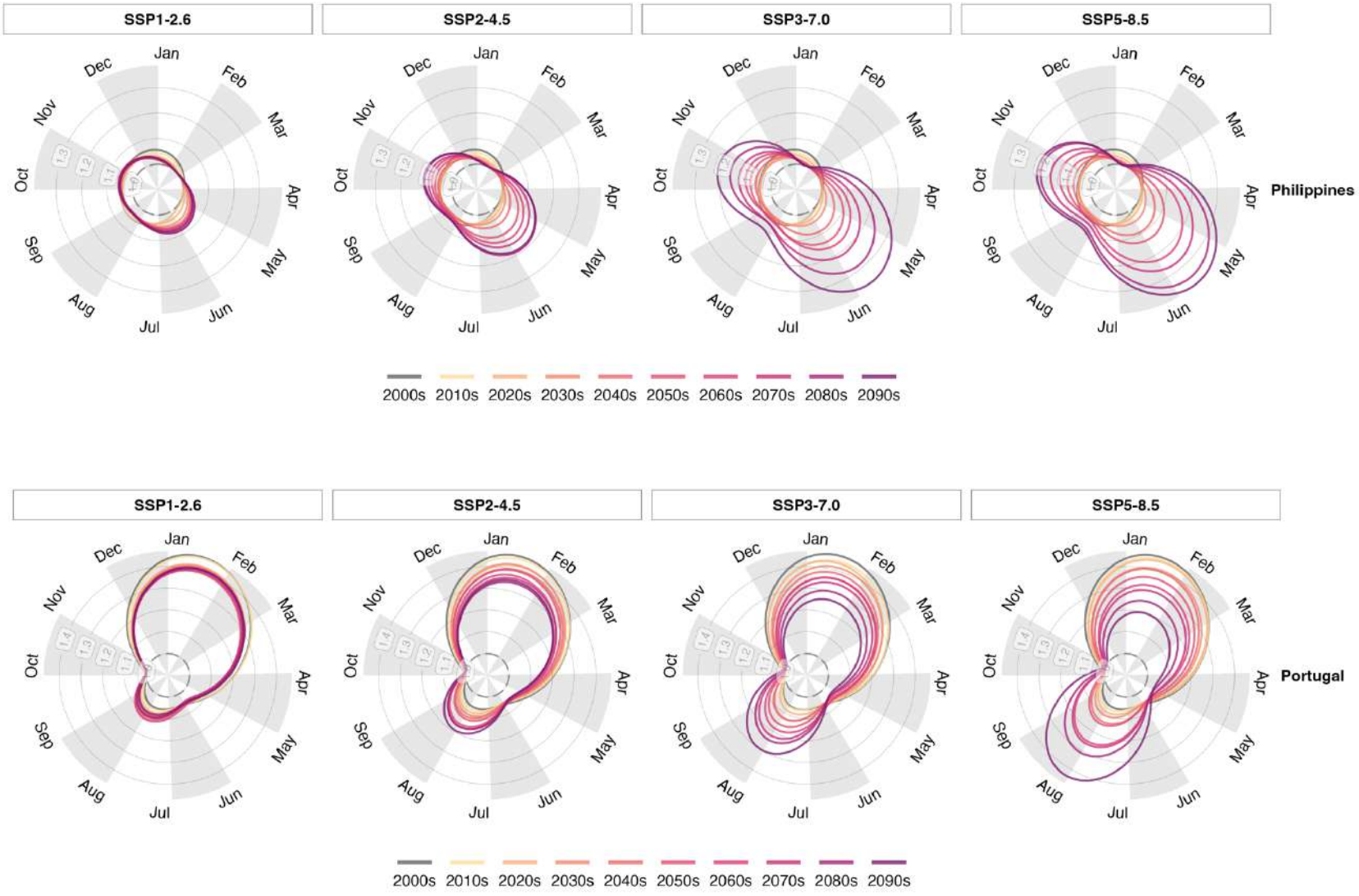
SSP1-2.6
SSP2-4.5
SSP3-7.0
SSP5-8.5
Jan
Feb
Mar
Apr
May
Jun
Jul
Aug
Sep
Oct
Nov
Dec
Philippines
Portugal
2000s
2010s
2020s
2030s
2040s
2050s
2060s
2070s
2080s
2090s

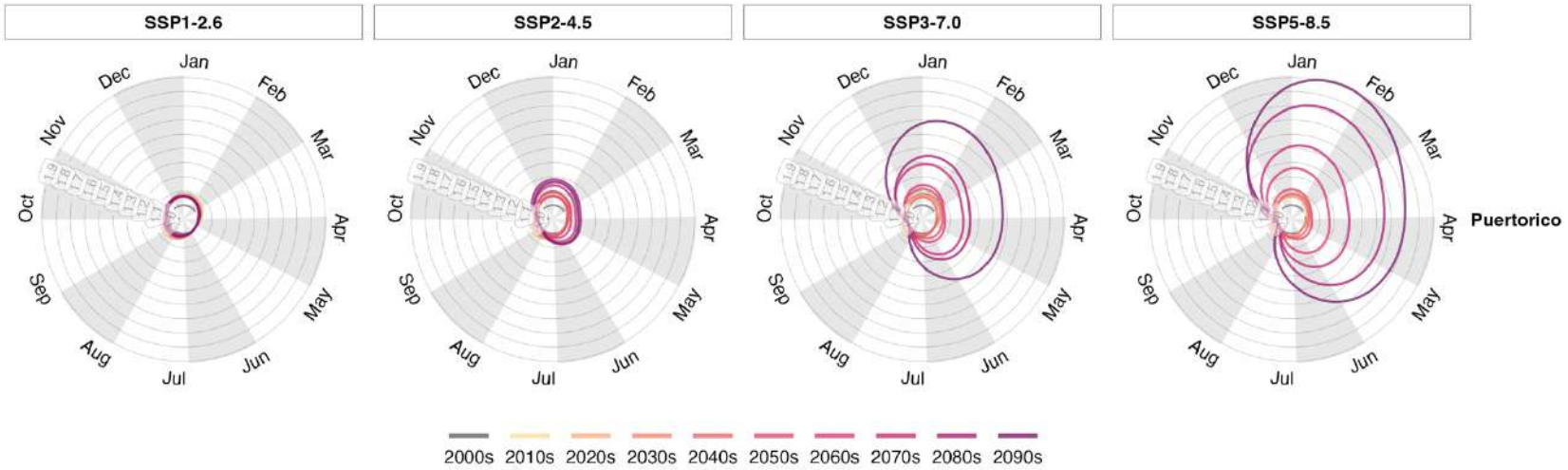
SSP1-2.6
SSP2-4.5
SSP3-7.0
SSP5-8.5
Jan
Feb
Mar
Apr
May
Jun
Jul
Aug
Sep
Oct
Nov
Dec
Puertorico
2000s
2010s
2020s
2030s
2040s
2050s
2060s
2070s
2080s
2090s

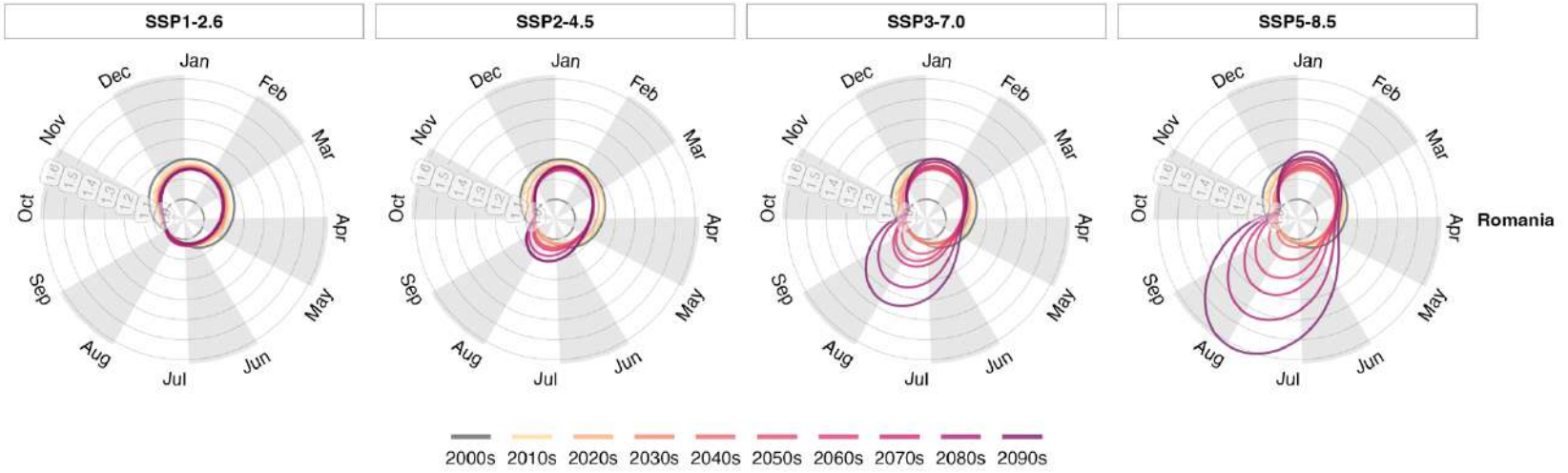
SSP1-2.6
SSP2-4.5
SSP3-7.0
SSP5-8.5
Jan
Feb
Mar
Apr
May
Jun
Jul
Aug
Sep
Oct
Nov
Dec
Romania
2000s
2010s
2020s
2030s
2040s
2050s
2060s
2070s
2080s
2090s

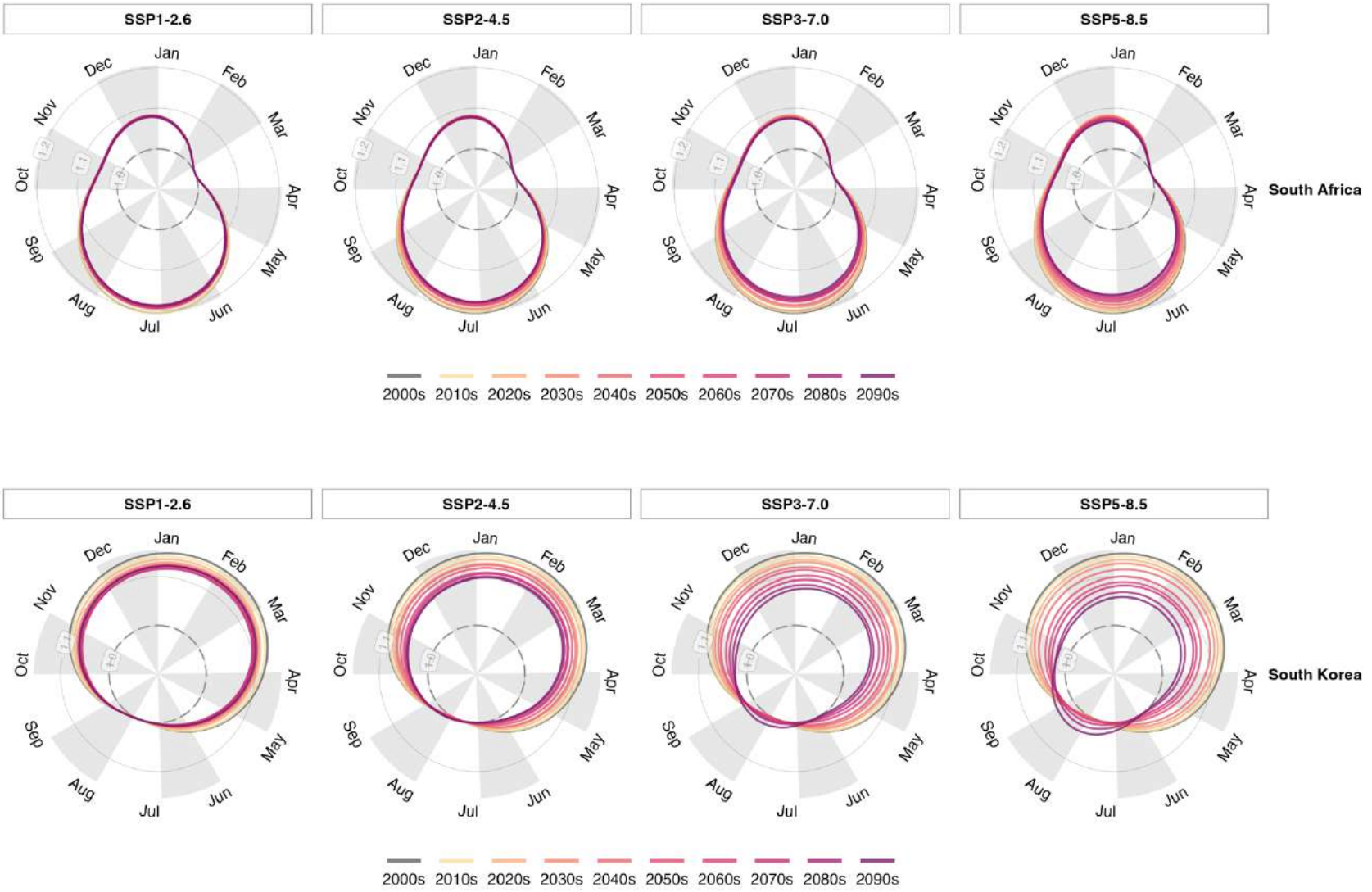
SSP1-2.6
SSP2-4.5
SSP3-7.0
SSP5-8.5
Jan
Feb
Mar
Apr
May
Jun
Jul
Aug
Sep
Oct
Nov
Dec
South Africa
South Korea
2000s
2010s
2020s
2030s
2040s
2050s
2060s
2070s
2080s
2090s

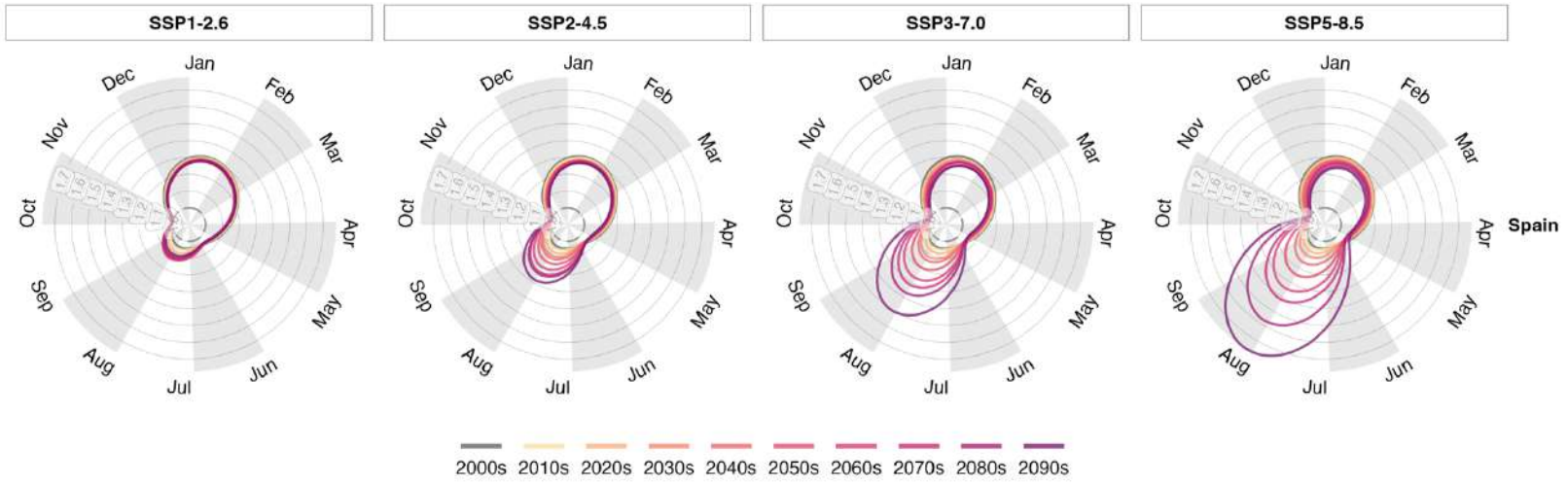
SSP1-2.6
SSP2-4.5
SSP3-7.0
SSP5-8.5
Spain
Jan
Feb
Mar
Apr
May
Jun
Jul
Aug
Sep
Oct
Nov
Dec
2000s
2010s
2020s
2030s
2040s
2050s
2060s
2070s
2080s
2090s

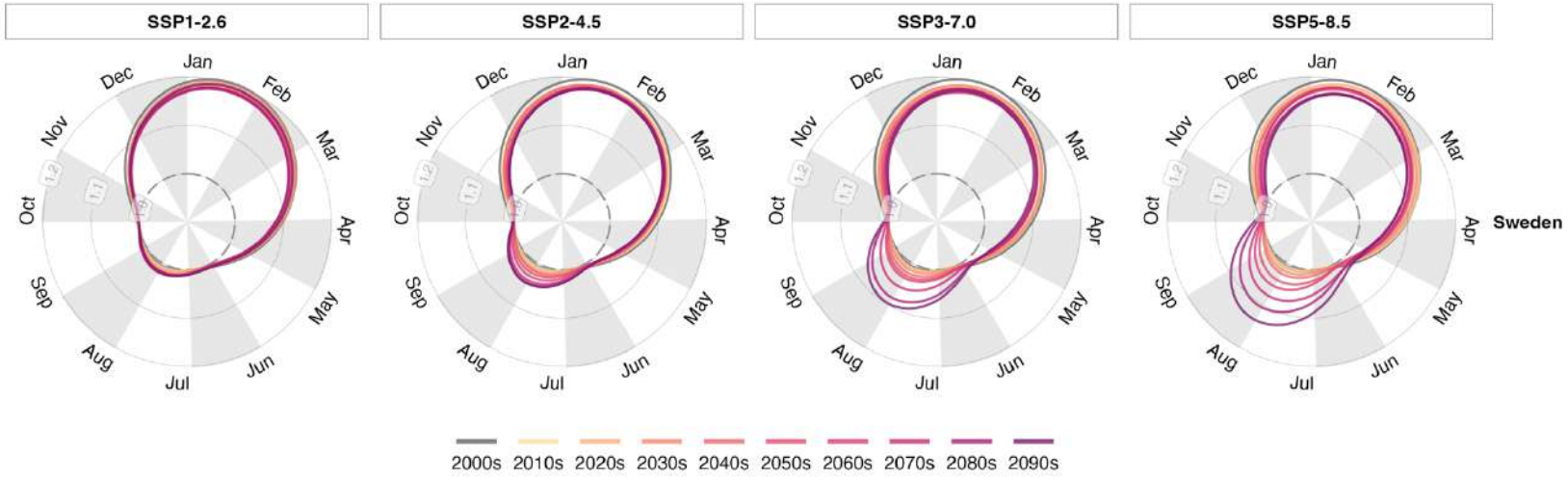
SSP1-2.6
SSP2-4.5
SSP3-7.0
SSP5-8.5
Sweden
Jan
Feb
Mar
Apr
May
Jun
Jul
Aug
Sep
Oct
Nov
Dec
2000s
2010s
2020s
2030s
2040s
2050s
2060s
2070s
2080s
2090s

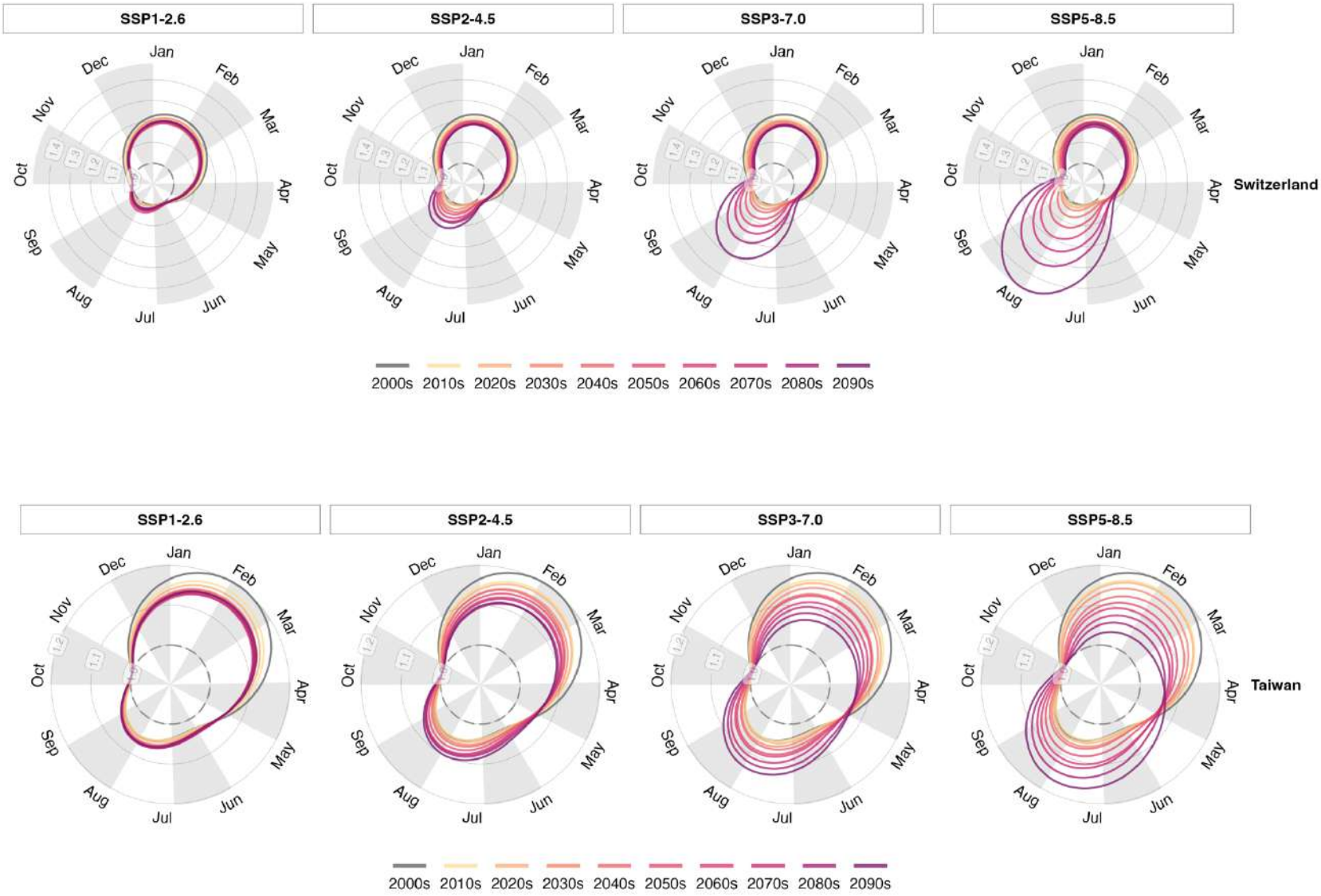
SSP1-2.6
SSP2-4.5
SSP3-7.0
SSP5-8.5
Switzerland
Taiwan
Jan
Feb
Mar
Apr
May
Jun
Jul
Aug
Sep
Oct
Nov
Dec
2000s
2010s
2020s
2030s
2040s
2050s
2060s
2070s
2080s
2090s

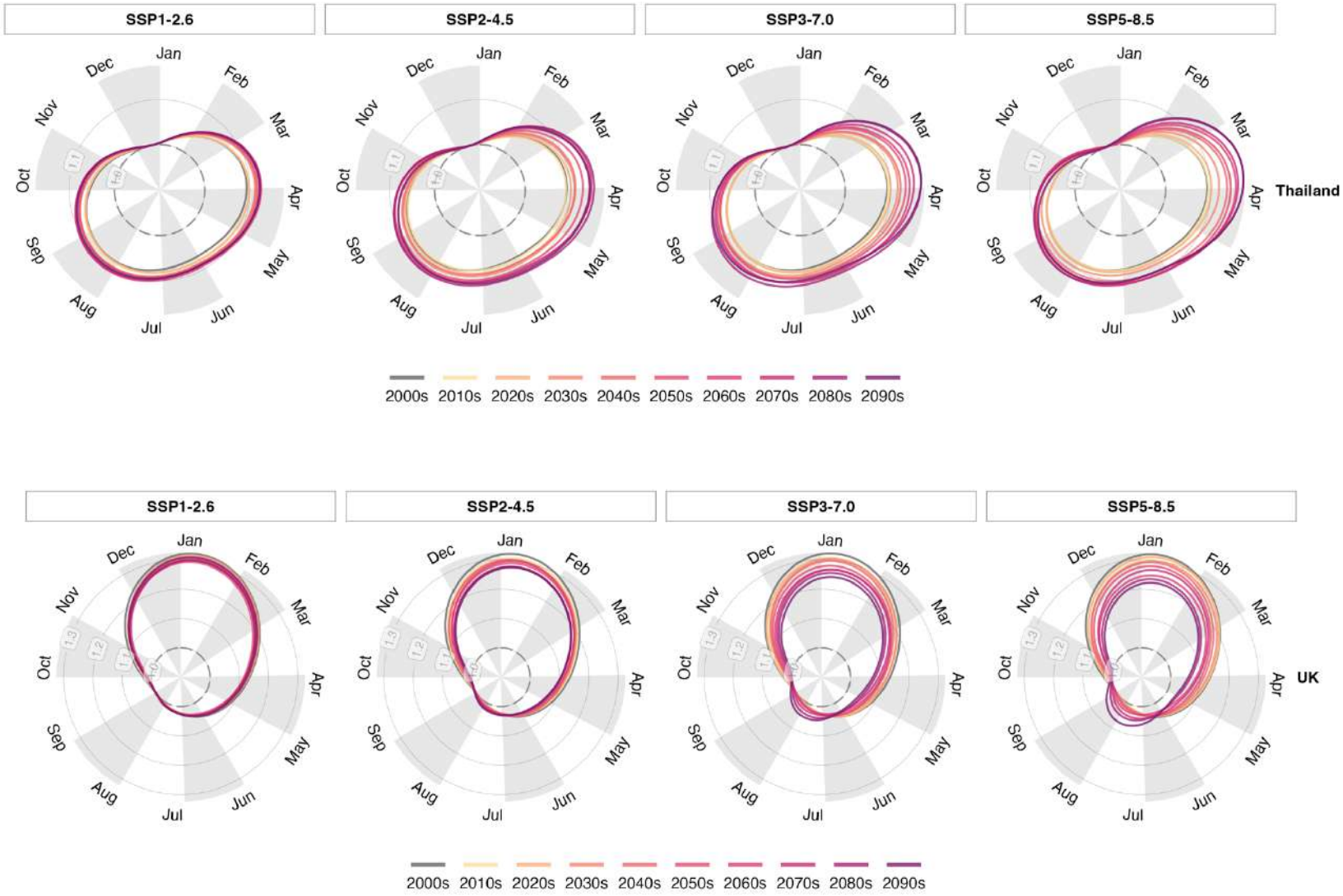
SSP1-2.6
SSP2-4.5
SSP3-7.0
SSP5-8.5
Jan
Feb
Mar
Apr
May
Jun
Jul
Aug
Sep
Oct
Nov
Dec
Thailand
2000s
2010s
2020s
2030s
2040s
2050s
2060s
2070s
2080s
2090s
SSP1-2.6
SSP2-4.5
SSP3-7.0
SSP5-8.5
UK
2000s
2010s
2020s
2030s
2040s
2050s
2060s
2070s
2080s
2090s

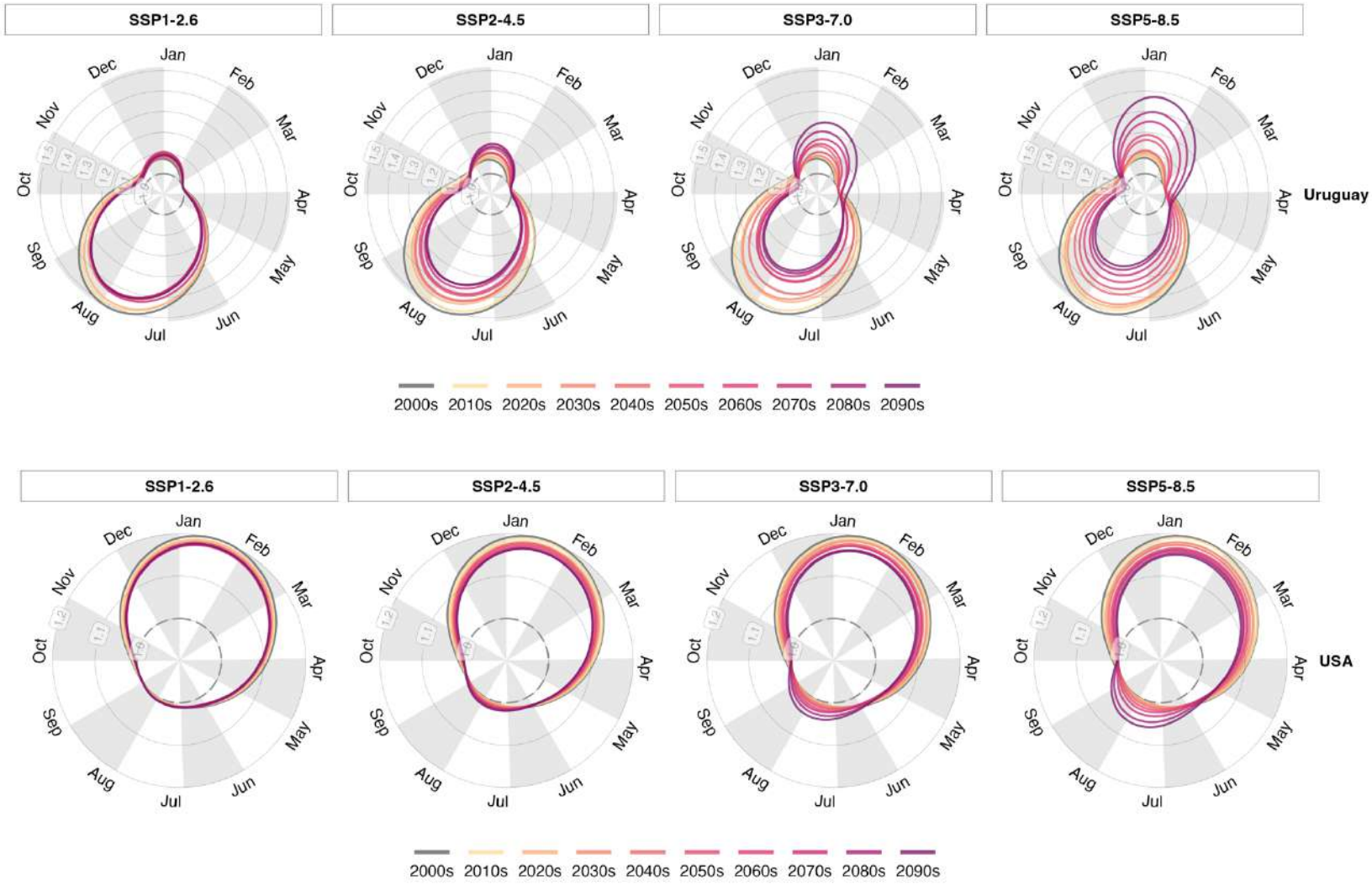
SSP1-2.6
SSP2-4.5
SSP3-7.0
SSP5-8.5
Uruguay
Jan
Feb
Mar
Apr
May
Jun
Jul
Aug
Sep
Oct
Nov
Dec
2000s
2010s
2020s
2030s
2040s
2050s
2060s
2070s
2080s
2090s
SSP1-2.6
SSP2-4.5
SSP3-7.0
SSP5-8.5
USA
Jan
Feb
Mar
Apr
May
Jun
Jul
Aug
Sep
Oct
Nov
Dec
2000s
2010s
2020s
2030s
2040s
2050s
2060s
2070s
2080s
2090s

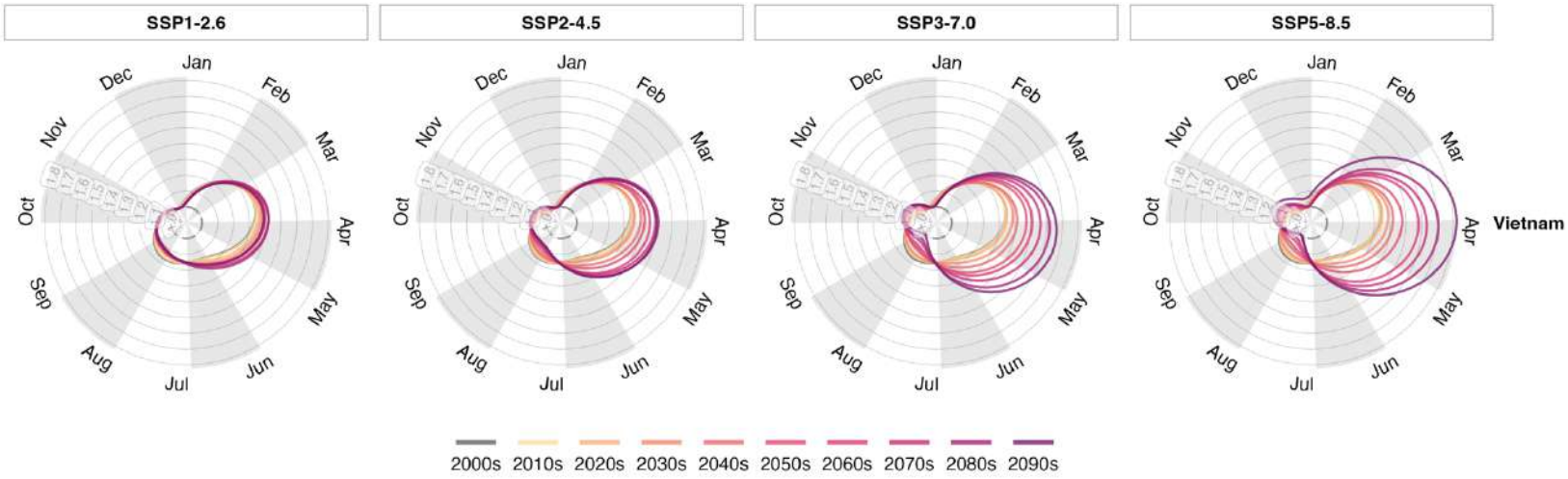
SSP1-2.6
SSP2-4.5
SSP3-7.0
SSP5-8.5
Jan
Feb
Mar
Apr
May
Jun
Jul
Aug
Sep
Oct
Nov
Dec
Vietnam
2000s
2010s
2020s
2030s
2040s
2050s
2060s
2070s
2080s
2090s

**Figure S2**. Temporal changes in the size of seasonality by country/area under four scenarios

The graph shows the difference in peak-to-trough ratio (PTR) and attributable fraction (AF) by decade compared with the 2000s in each country/area.
Change in PTR and AF is calculated as the ratio of PTR and the absolute difference in AF by decade compared with the 2000s, respectively.
The colour of the lines represents different scenarios.

**Note:** The two polar locations in Peru were included when pooling the results for Peru.

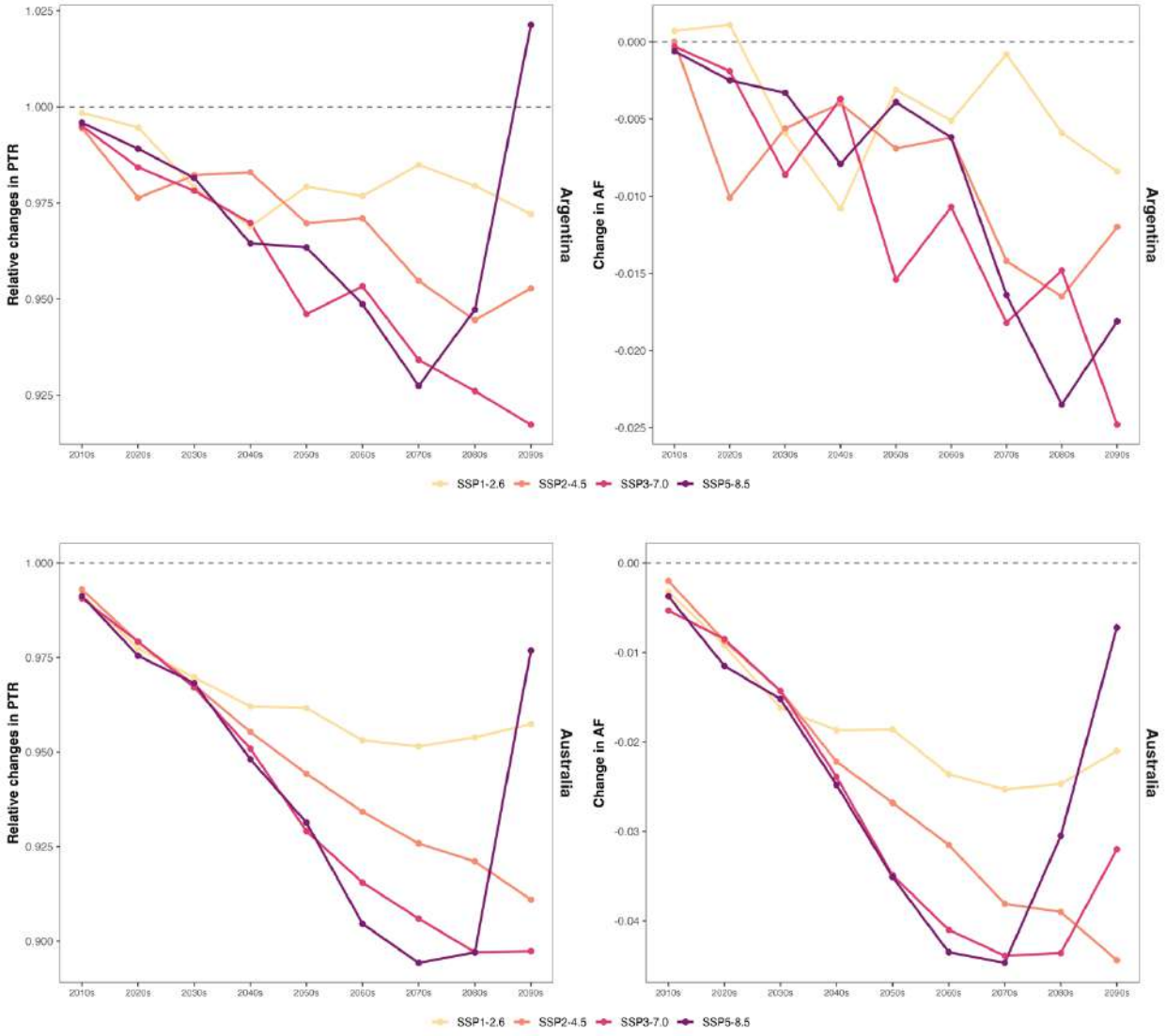
Relative changes in PTR
Change in AF
Argentina
Australia
SSP1-2.6
SSP2-4.5
SSP3-7.0
SSP5-8.5

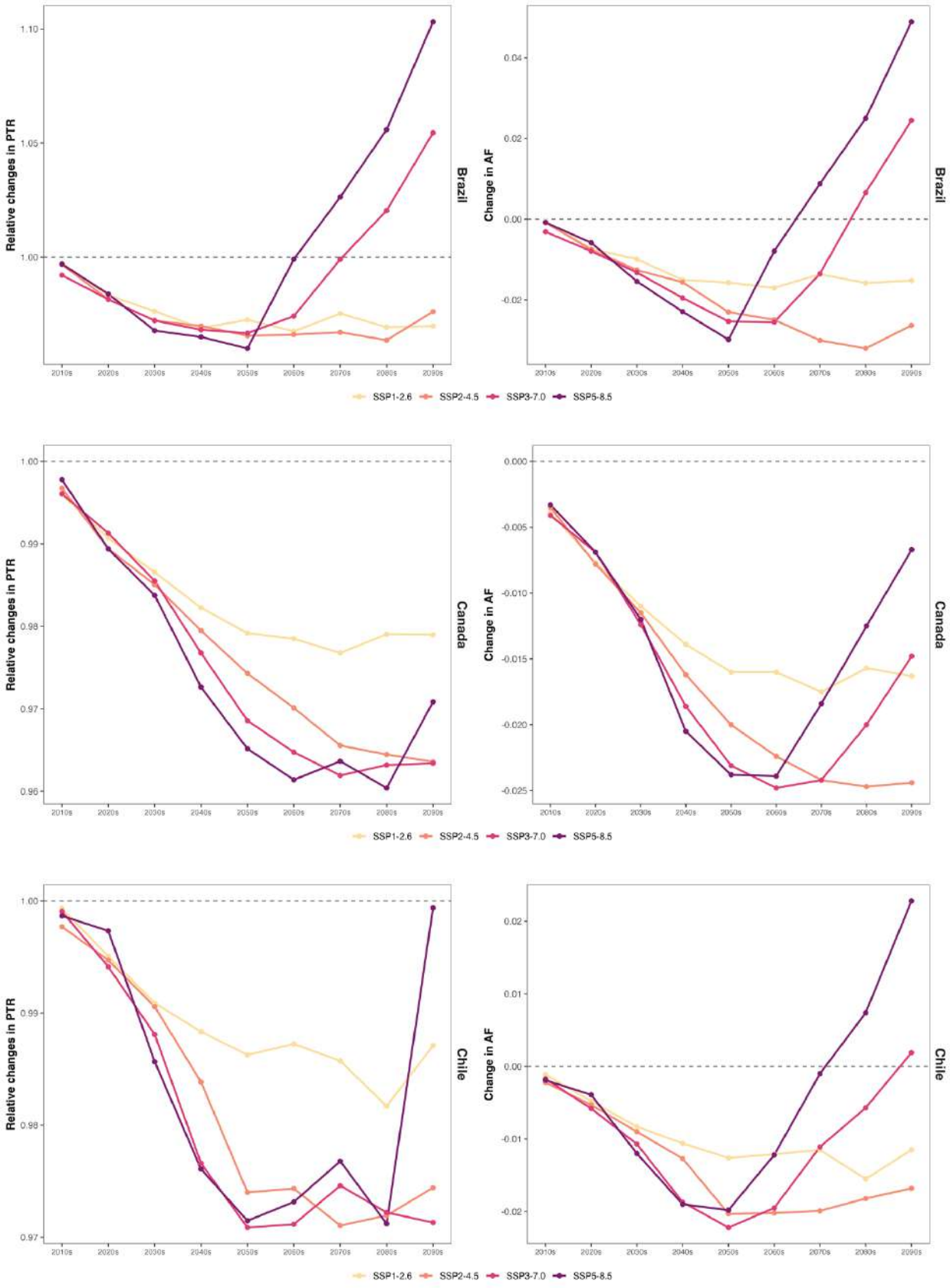
Relative changes in PTR
Change in AF
Brazil
Canada
Chile
2010s
2020s
2030s
2040s
2050s
2060s
2070s
2080s
2090s
SSP1-2.6
SSP2-4.5
SSP3-7.0
SSP5-8.5

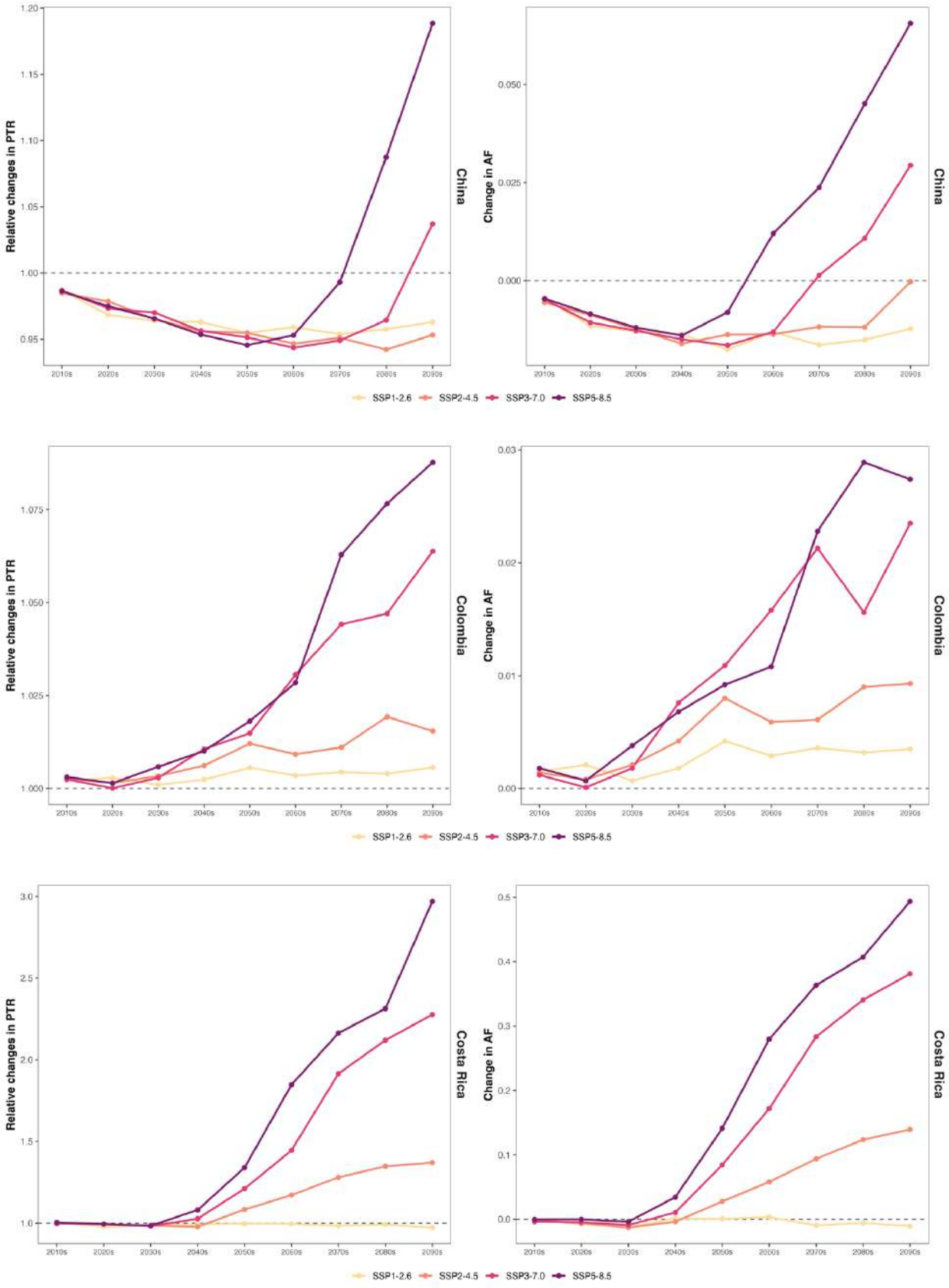
Relative changes in PTR
Change in AF
China
Colombia
Costa Rica
2010s
2020s
2030s
2040s
2050s
2060s
2070s
2080s
2090s
SSP1-2.6
SSP2-4.5
SSP3-7.0
SSP5-8.5

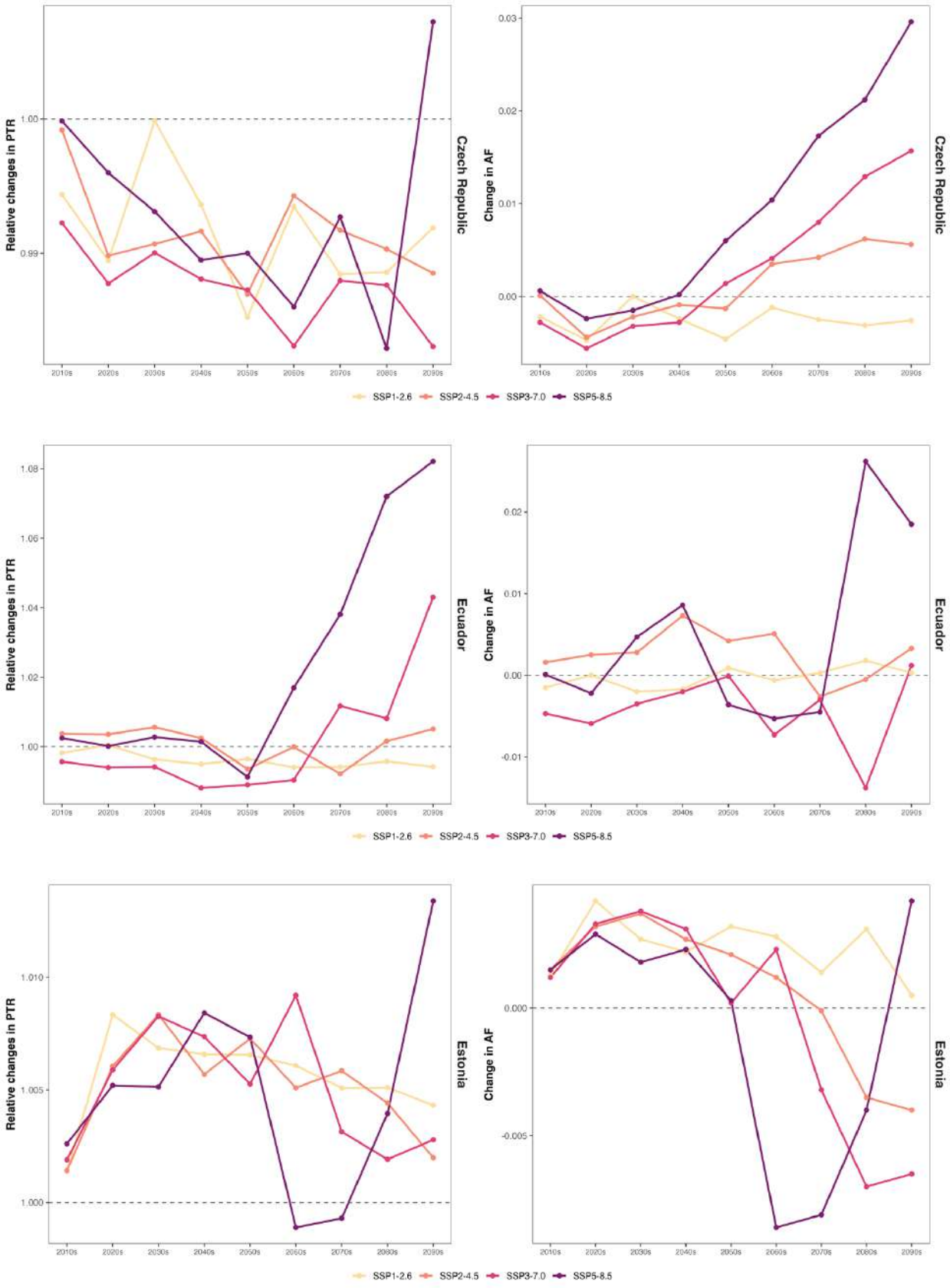
Relative changes in PTR
Change in AF
Czech Republic
Ecuador
Estonia
2010s
2020s
2030s
2040s
2050s
2060s
2070s
2080s
2090s
SSP1-2.6
SSP2-4.5
SSP3-7.0
SSP5-8.5

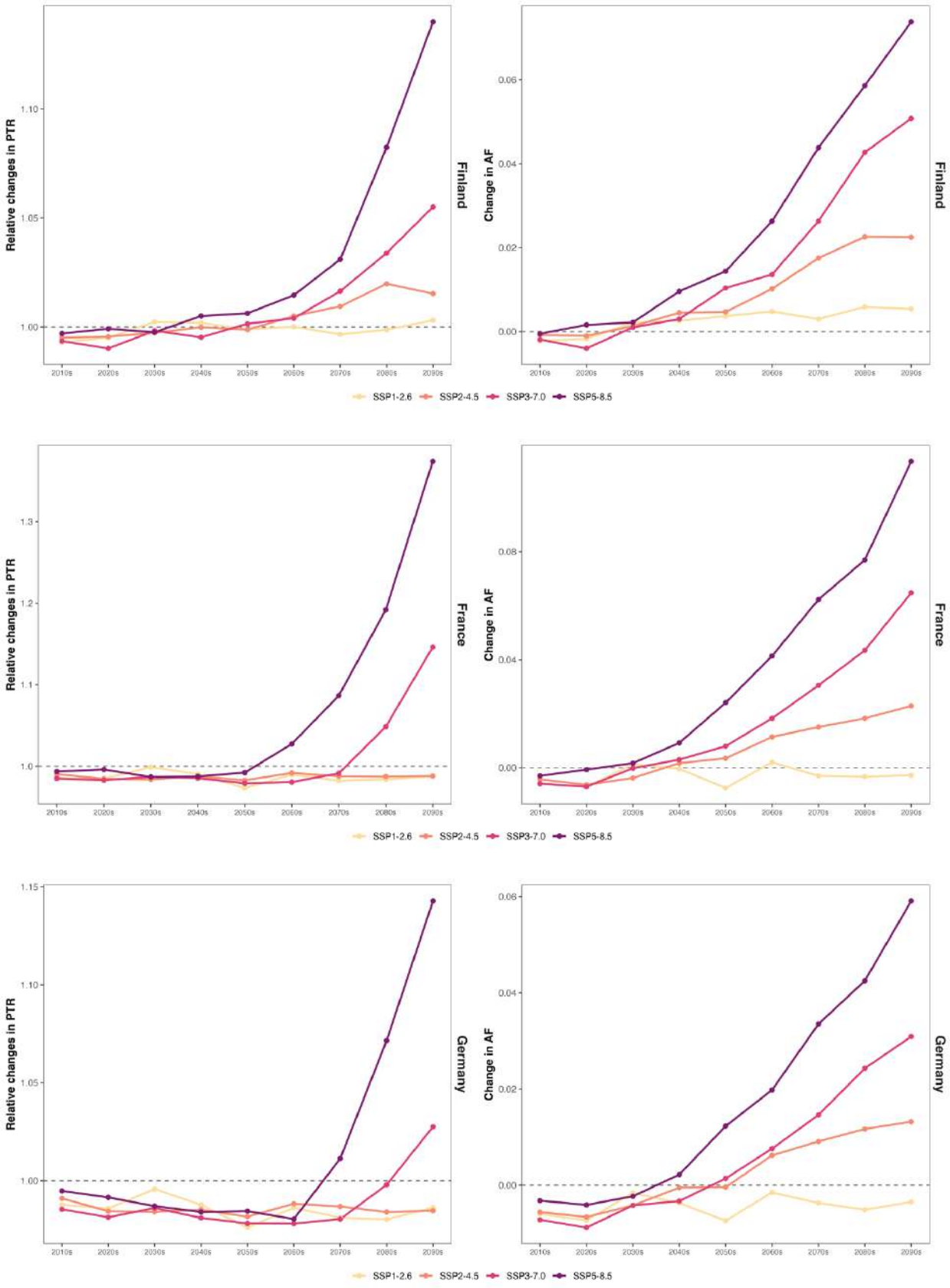
Relative changes in PTR
Change in AF
Finland
France
Germany
SSP1-2.6
SSP2-4.5
SSP3-7.0
SSP5-8.5

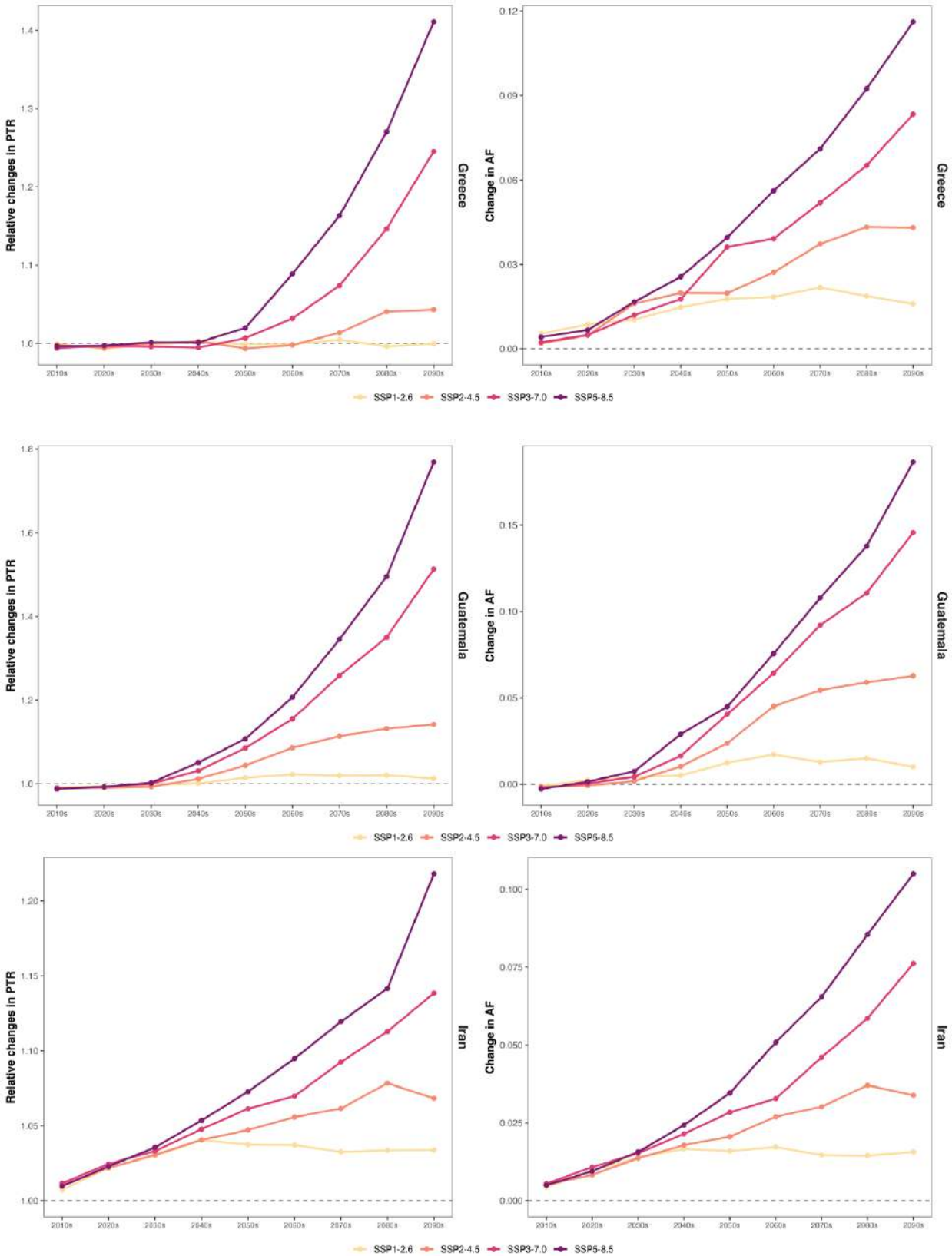
Relative changes in PTR
Change in AF
Greece
Guatemala
Iran
2010s
2020s
2030s
2040s
2050s
2060s
2070s
2080s
2090s
SSP1-2.6
SSP2-4.5
SSP3-7.0
SSP5-8.5

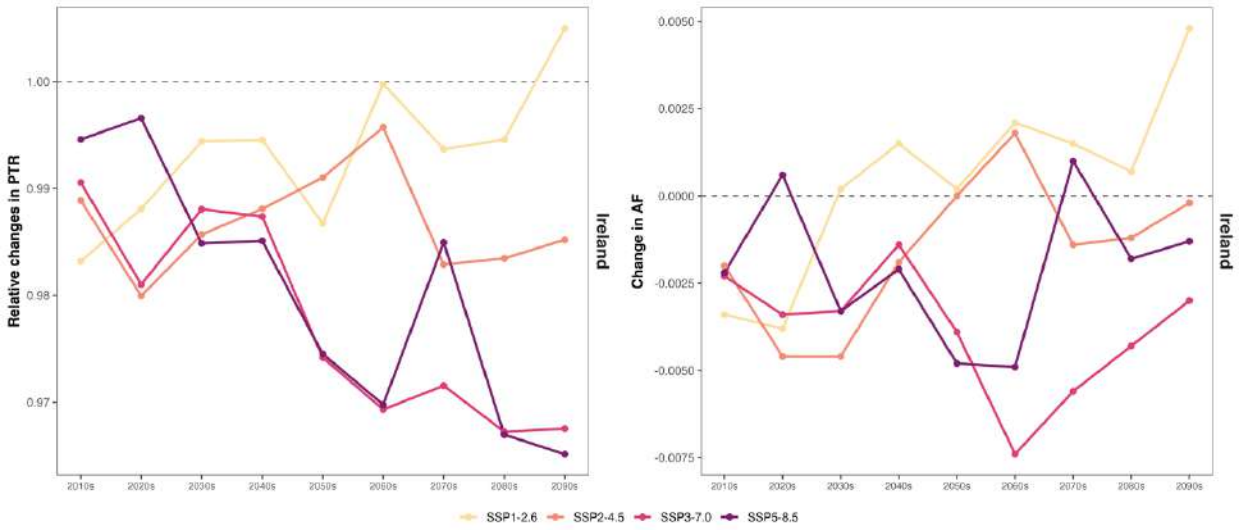
Relative changes in PTR
1.00
0.99
0.98
0.97
2010s
2020s
2030s
2040s
2050s
2060s
2070s
2080s
2090s
Ireland
Change in AF
0.0050
0.0025
0.0000
-0.0025
-0.0050
-0.0075
Ireland
SSP1-2.6
SSP2-4.5
SSP3-7.0
SSP5-8.5

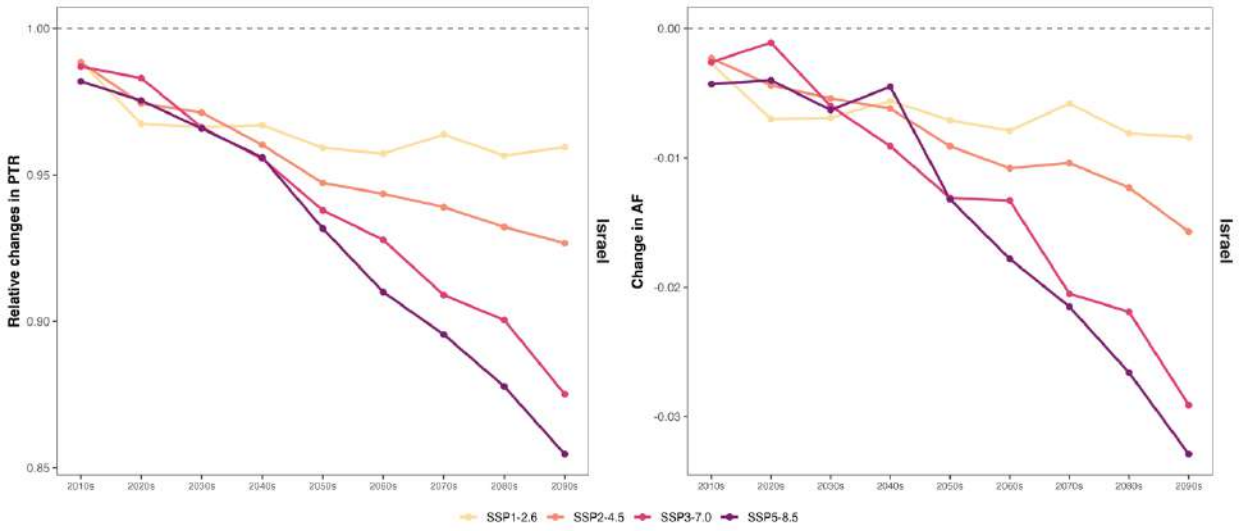
Relative changes in PTR
1.00
0.95
0.90
0.85
2010s
2020s
2030s
2040s
2050s
2060s
2070s
2080s
2090s
Israel
Change in AF
0.00
-0.01
-0.02
-0.03
Israel
SSP1-2.6
SSP2-4.5
SSP3-7.0
SSP5-8.5

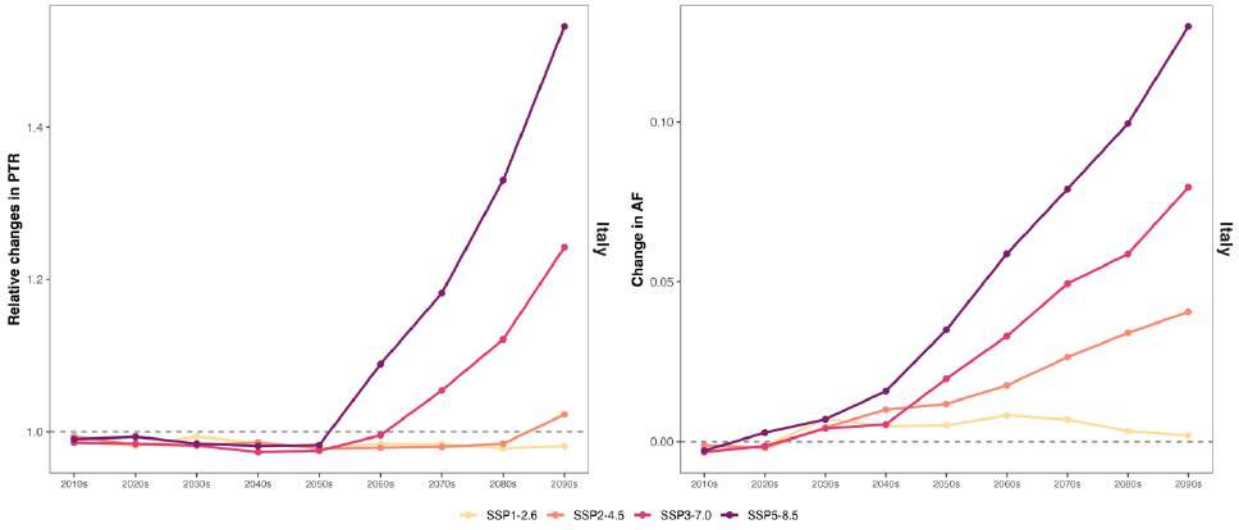
Relative changes in PTR
1.4
1.2
1.0
2010s
2020s
2030s
2040s
2050s
2060s
2070s
2080s
2090s
Italy
Change in AF
0.10
0.05
0.00
Italy
SSP1-2.6
SSP2-4.5
SSP3-7.0
SSP5-8.5

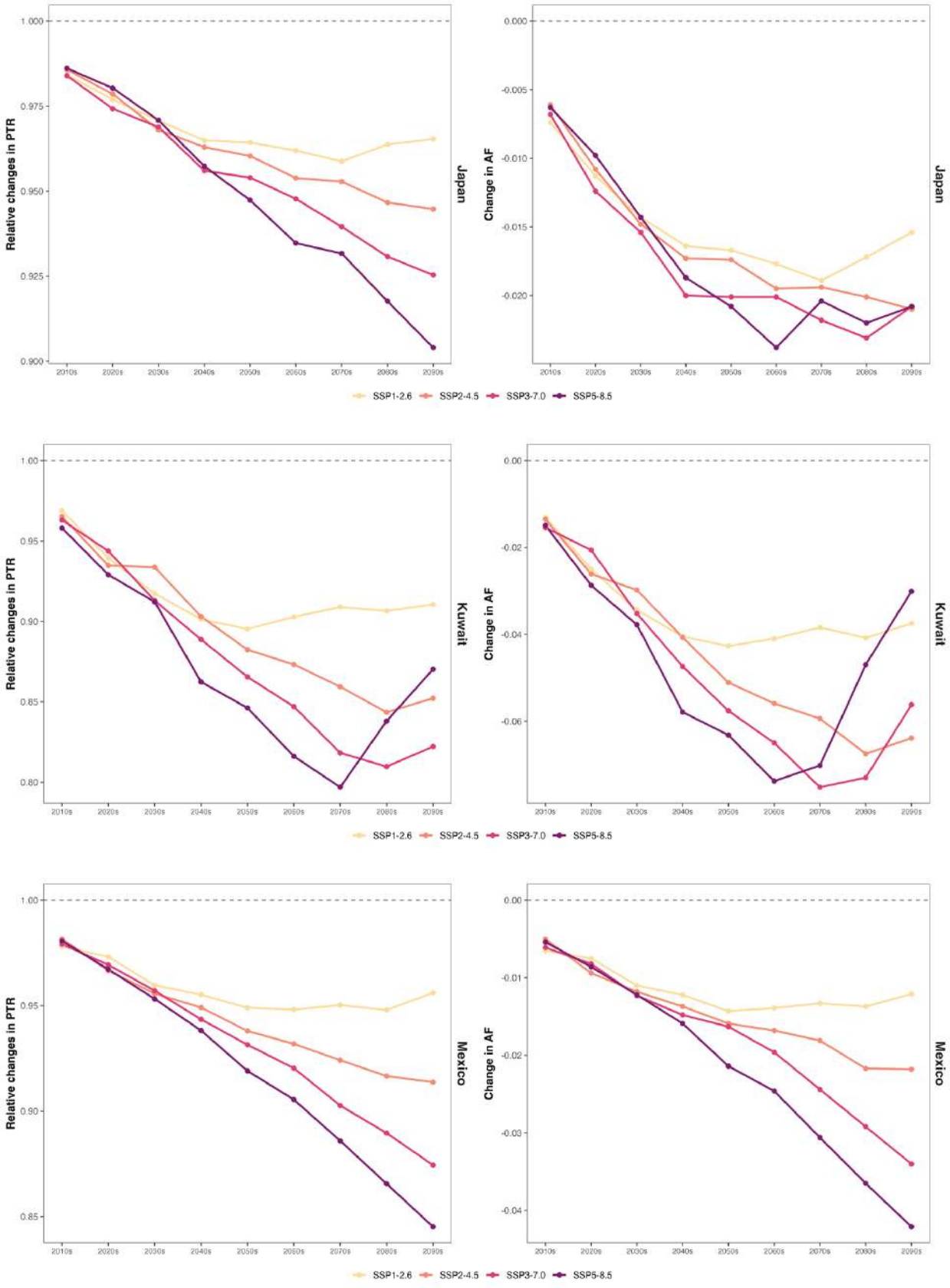
Relative changes in PTR
Change in AF
Japan
Kuwait
Mexico
SSP1-2.6
SSP2-4.5
SSP3-7.0
SSP5-8.5

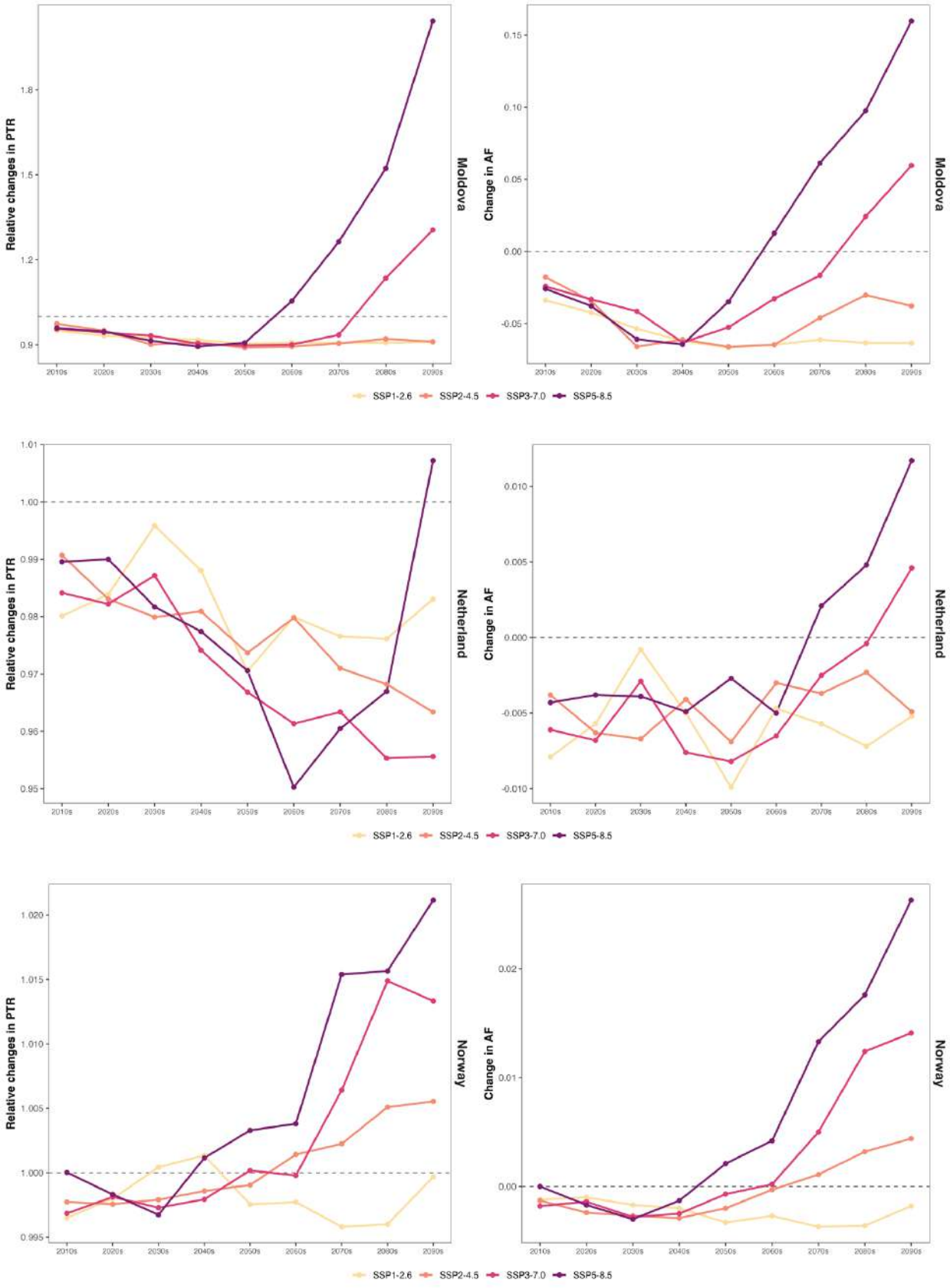
Relative changes in PTR
Change in AF
Moldova
Netherland
Norway
2010s
2020s
2030s
2040s
2050s
2060s
2070s
2080s
2090s
SSP1-2.6
SSP2-4.5
SSP3-7.0
SSP5-8.5

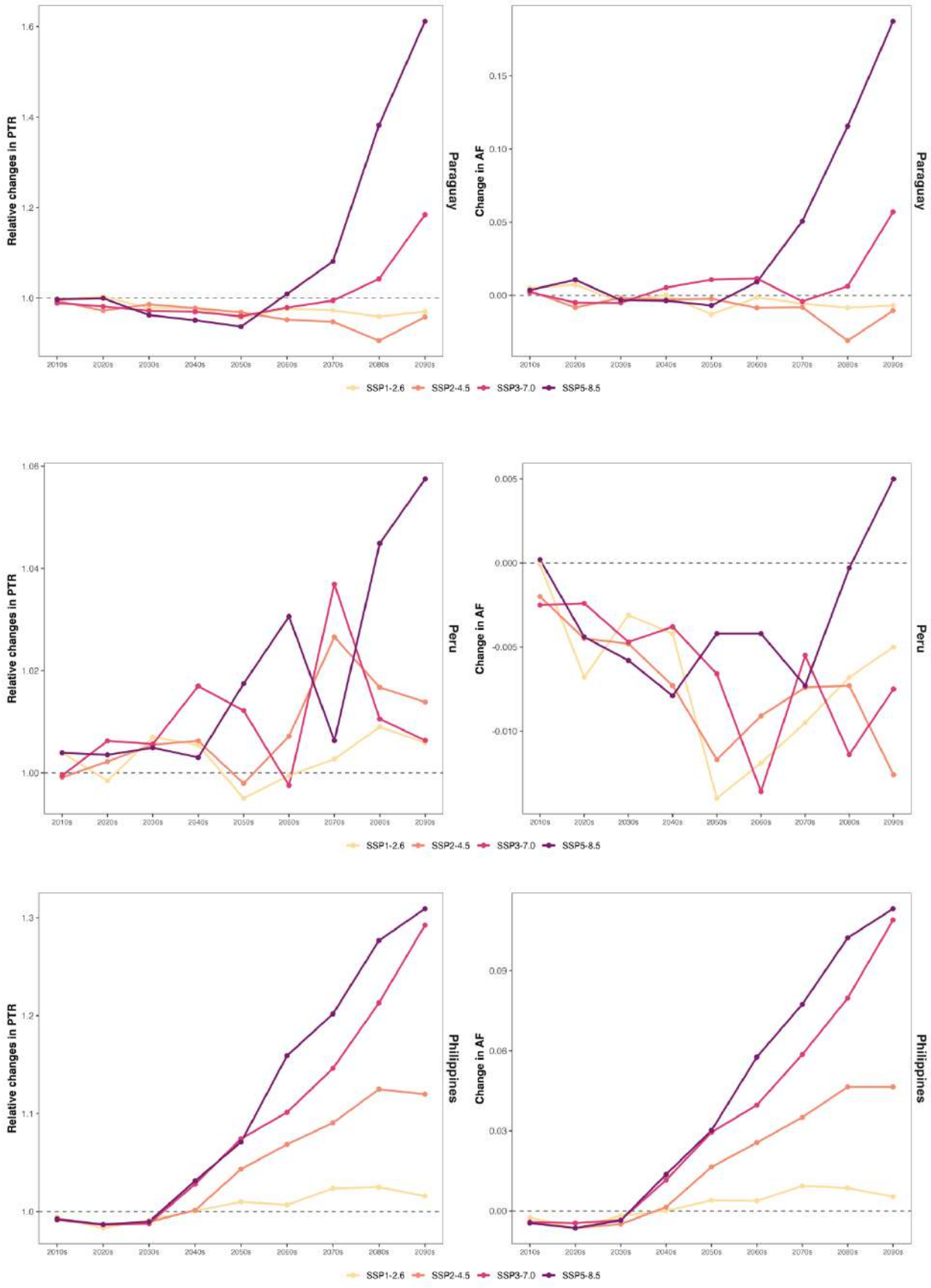
Relative changes in PTR
Change in AF
Paraguay
Peru
Philippines
2010s
2020s
2030s
2040s
2050s
2060s
2070s
2080s
2090s
SSP1-2.6
SSP2-4.5
SSP3-7.0
SSP5-8.5

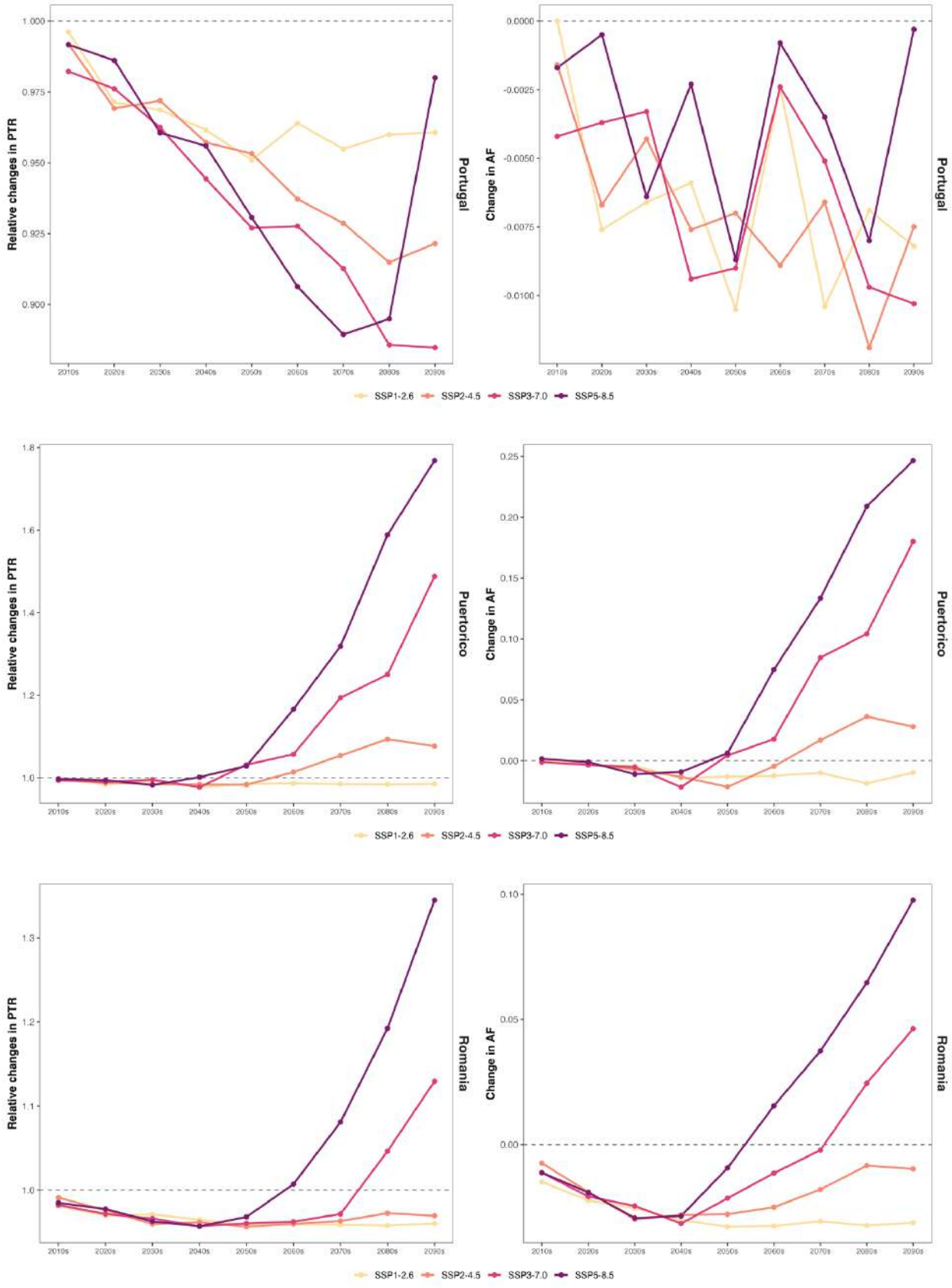
Relative changes in PTR
Change in AF
Portugal
Puertorico
Romania
SSP1-2.6
SSP2-4.5
SSP3-7.0
SSP5-8.5

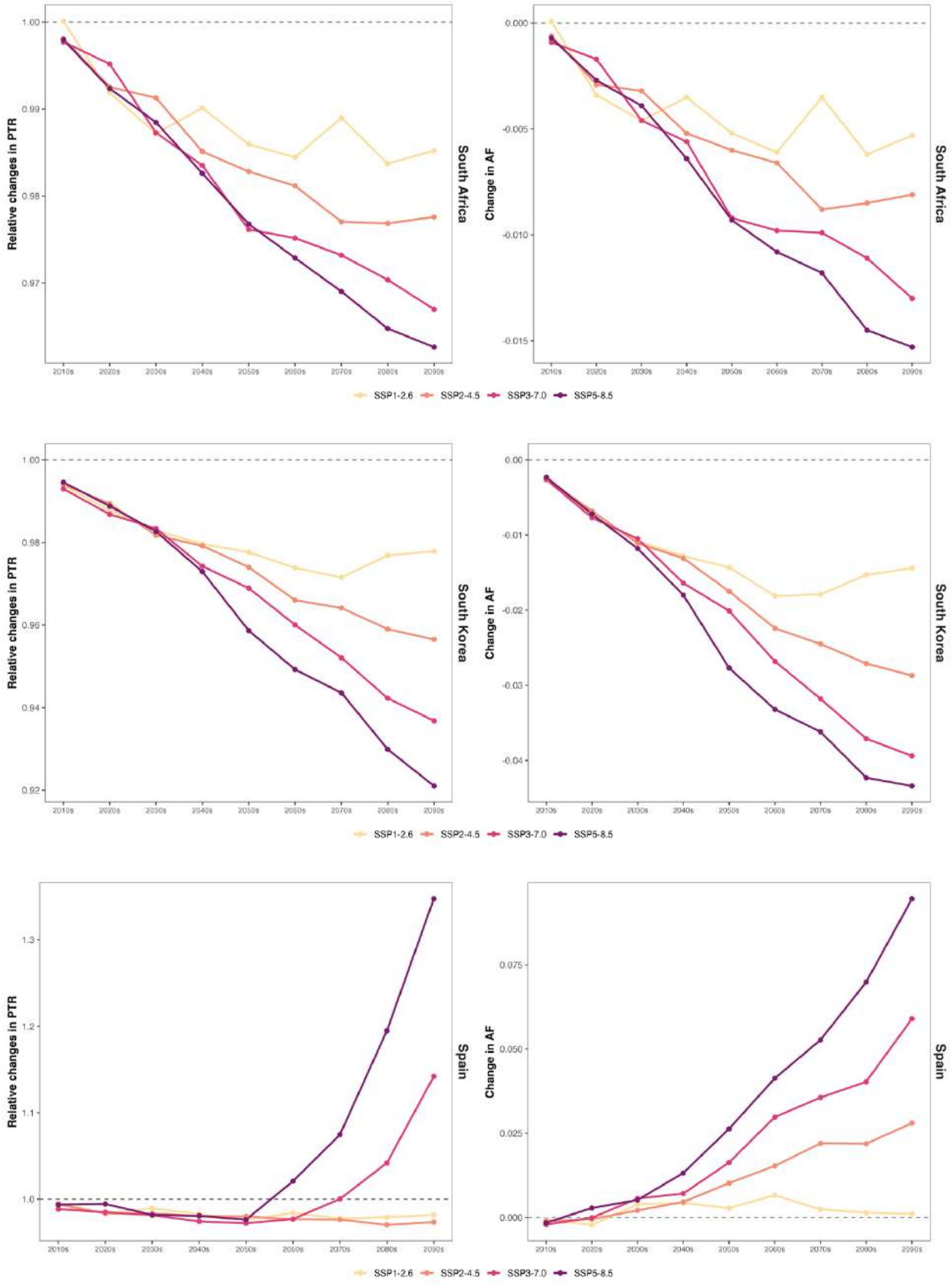
Relative changes in PTR
Change in AF
South Africa
South Korea
Spain
SSP1-2.6
SSP2-4.5
SSP3-7.0
SSP5-8.5

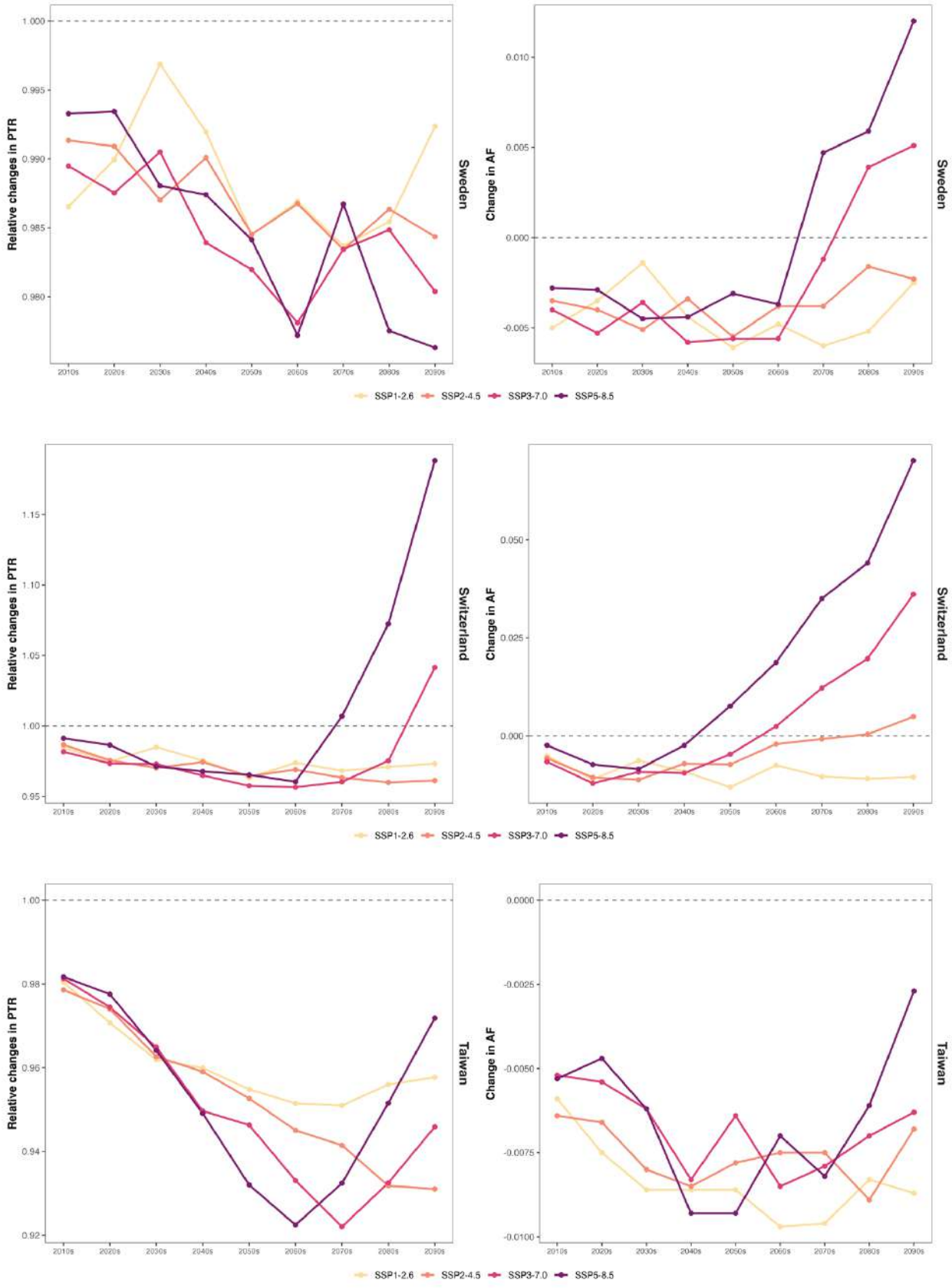
Relative changes in PTR
Change in AF
Sweden
Switzerland
Taiwan
2010s
2020s
2030s
2040s
2050s
2060s
2070s
2080s
2090s
SSP1-2.6
SSP2-4.5
SSP3-7.0
SSP5-8.5

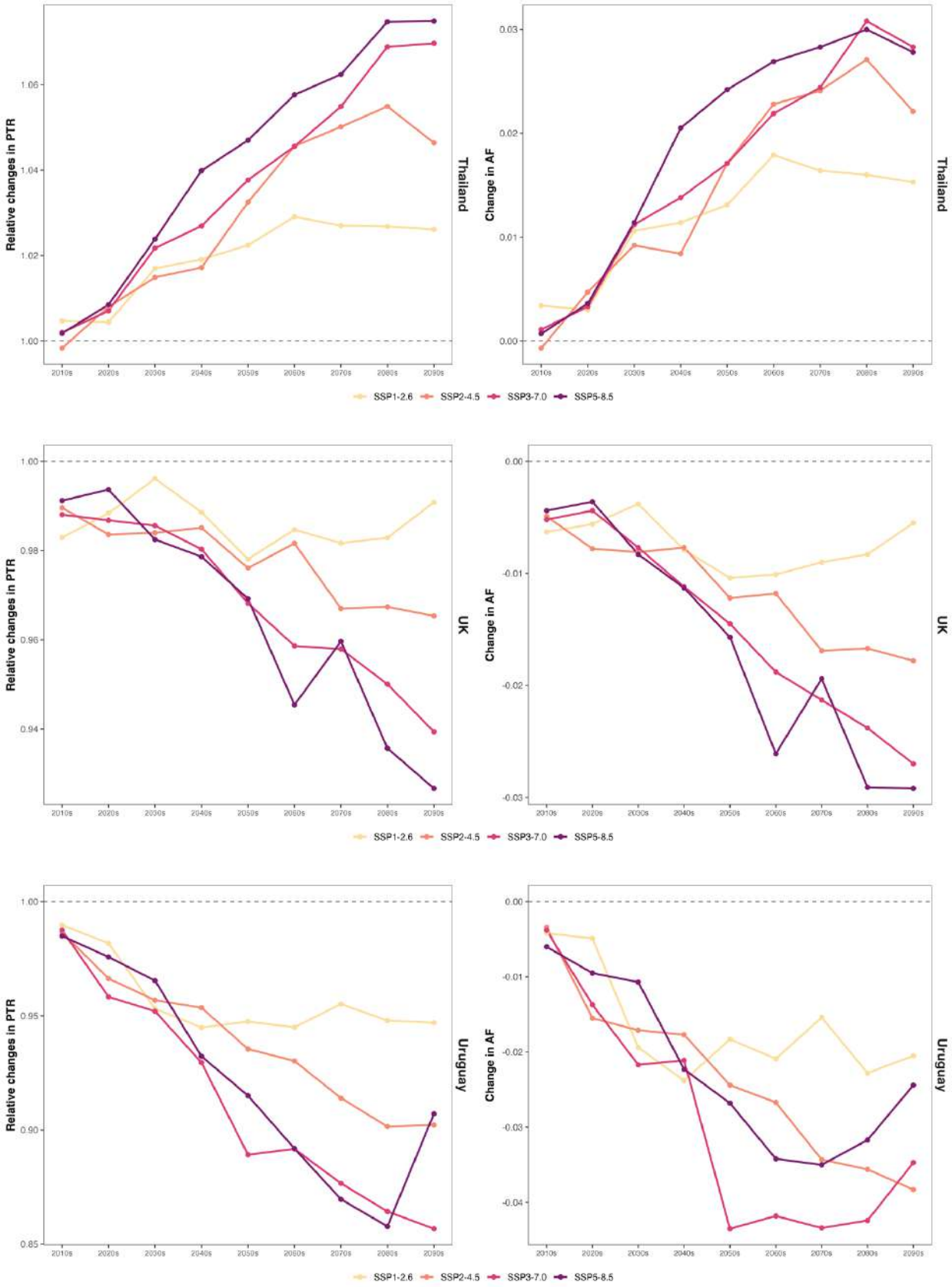
Relative changes in PTR
Change in AF
Thailand
UK
Uruguay
SSP1-2.6
SSP2-4.5
SSP3-7.0
SSP5-8.5

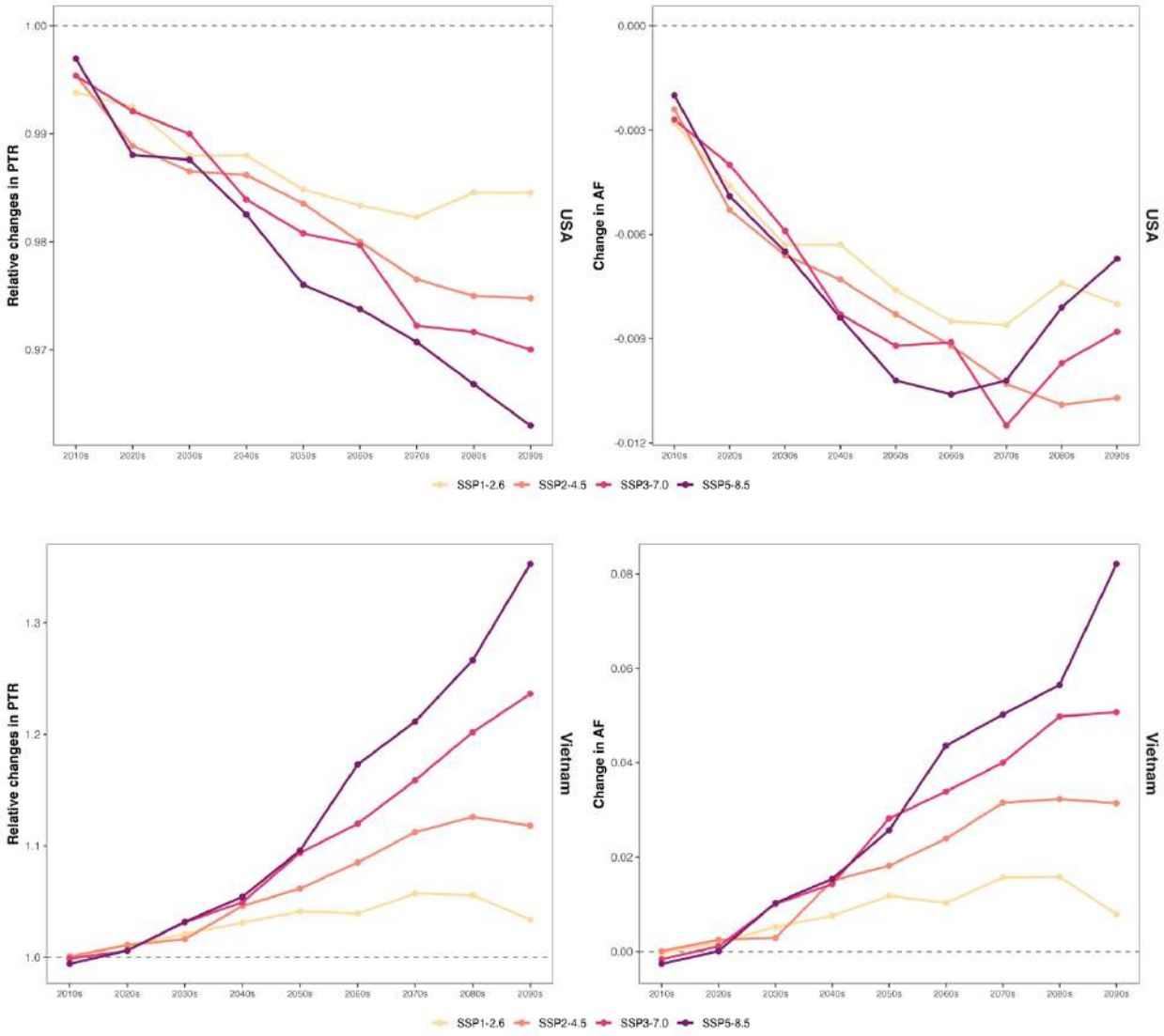
Relative changes in PTR
Change in AF
USA
Vietnam
SSP1-2.6
SSP2-4.5
SSP3-7.0
SSP5-8.5